

3D MODEL ANALYSIS OF HUMAN FOOT

A Thesis Submitted in Partial Fulfillment
of the Requirements for the Degree of
Bachelor of Technology

in

Biomedical Engineering

by

UMAKANTA NAYAK

110BM0012

Under the supervision of

Dr. A. THIRUGNANAM



Department of Biotechnology & Medical Engineering

National Institute of Technology

Rourkela, Odisha-769008

May 2014



**Department of Biotechnology and Medical Engineering
National Institute of Technology Rourkela,
Odisha 769008, India**

CERTIFICATE

This is to certify that the report entitled “**3D MODEL ANALYSIS OF HUMAN FOOT**” being submitted by **UMAKANTA NAYAK (Roll No 110BM0012)** towards the fulfillment of the requirement for the degree of Bachelors of Technology in Biomedical Engineering at Department of Biotechnology & Medical Engineering, NIT Rourkela is a record of bonafide work carried out by him under my guidance and supervision.

Rourkela

Date:

Dr. A. THIRUGNANAM

Dept. of Biotechnology and Medical Engineering
National Institute of Technology Rourkela

ACKNOWLEDGEMENT

I feel immense pleasure and privilege in expressing my deep gratitude, in indebtedness and thankfulness towards all the people who have helped, inspired and encouraged me during the preparation of this report.

I would like to thank **Dr. A. Thirugnanam**, who provided me this opportunity to highlight the key aspects of an upcoming technology and guided me during the project work preparation. I place on record my sincere gratitude to **Prof. Krishna Pramanik**, Head of Department, Department of Biotechnology and Medical Engineering, NIT Rourkela for her constant encouragement.

I would like to thank **Ms. Reshmi Dey**, **Mr. Krishna Kumar Ramajayam** and **Mr. Shreshan Jena**, Ph.D Scholars, Department of Biotechnology and Medical Engineering, NIT Rourkela, **Mr. Patitapabana Parida**, and my friends **Mr. Bijay Kumar Debata** and **Mr. Kumar Prabhu Kalyan** for their regular support, help and motivation.

Last but not the least, I would like to thank whole heartedly my parents and family members whose love and unconditional support, both on academic and personal front, enabled me to see the light of this day.

UMAKANTA NAYAK

110BM0012

CONTENTS

TABLE OF CONTENTS	PAGE NO
ABBREVIATIONS	iv
LIST OF FIGURES	v
LIST OF TABLES	vii
ABSTRACT	1
CHAPTER 1	2
1.0 INTRODUCTION	3
1.1 3D MODELING	3
1.2 FINITE ELEMENT ANALYSIS FOOT BONE	4
1.3 BIOMECHANICS OF FOOT	6
1.4 ANATOMY AND BIOMECHANICS OF THE FOOT	7
CHAPTER 2	11
2.0 INTRODUCTION	12
2.1 3D MODELLING	12
2.2 FINITE ELEMENT MODELING	14
2.3 OBJECTIVES	14
CHAPTER 3	15
3.0 METHODS	16
3.1 COMBINING THE CT SCAN IMAGE SEQUENCE	17
3.2 3D RECONSTRUCTION	18
3.3 CLEANING OF THE MODEL	18
3.4 CONVERTING INTO ANSYS FILE FORMAT	18

3.5 IMPORTING THE MODEL INTO ANSYS	19
3.6 MESHING	19
3.7 ANALYSIS – DEFORMATION	19
CHAPTER 4	20
4.0 RESULTS AND DISCUSSIONS	21
4.1 CT-SCAN IMAGE SEQUENCE	22
4.2 3-D IMAGE CONSTRUCTION	22
4.3 CLEANING, REPAIRING, SIZE REDUCTION AND SMOOTHING	24
4.4 ANSYS ANALYSIS	25
5.0 SUMMARY AND CONCLUSION	37
REFERENCES	38

ABBREVIATIONS & SYMBOLS

1. FEA	-	Finite element analysis
2. FEM	-	Finite element model
3. CT	-	Computed tomography
4. MRI	-	Magnetic resonance imaging
5. CAD	-	Computer aided design
6. 2D	-	Two dimension
7. 3D	-	Three dimension
8. GRF	-	Ground reaction force
9. COG	-	Center of gravity
10. ν	-	Poisson's ratio
11. UTS	-	Ultimate tensile strength
12. σ	-	Stress
13. ΔL	-	Change in length
14. M	-	Mass
15. A	-	Acceleration
16. F	-	Force

LIST OF FIGURES

PAGE NO

Fig. 1.1	Human foot bone model	4
Fig. 1.2	Computational methods to analyze the physical system	5
Fig. 1.3	Different element types	6
Fig. 1.4	Anatomy of the foot	7
Fig. 1.5	Different foot strike patterns	8
Fig. 1.6	Anglevariation of between different foot strikes	9
Fig. 1.7	Foot strike close to COG	9
Fig. 1.8	Three types of plane of foot	10
Fig. 1.9	Segmentation of a human foot from individual coronal CT slices	10
Fig. 2.1	Different geometric models (a) wireframe model,(b) surface model and (c) solid model	12
Fig. 3.1	Schematic diagram showing the FEM generation	17
Fig. 4.1	Results of the Snap shot of various softwares	21
Fig. 4.2	Combined CT scan images	22
Fig. 4.3	The details of the grayscale image	23
Fig. 4.4	The three sectional view of ITK SNAP	23
Fig. 4.5	Constructed 3D model of human foot bone	24
Fig. 4.6	Final model of foot boneafter cleaning	24
Fig. 4.7	Converting the .STL file format to .IGS for ANSYS using solid works	25
Fig. 4.8	Screenshot of model after import into ANSYS	25
Fig. 4.9	Screenshot of the messed foot model in ANSYS	26
Fig. 4.10	Screenshot of total deformation of foot model by applying 600N at an angle of 90^0	27
Fig. 4.11	Screenshot of total deformation of foot model by applying 700N at an angle of 90^0	27
Fig. 4.12	Screenshot of total deformation of foot model by applying 800N at an angle of 90^0	28
Fig. 4.13	Screenshot of total deformation of foot model by applying 600N at an angle 120^0	28
Fig. 4.14	Screenshot of total deformation of foot model by applying 700N	29

	at an angle 120°	
Fig. 4.15	Screenshot of total deformation of foot model by applying 800N at an angle 120°	29
Fig. 4.16	Screenshot of total deformation of foot model by applying 600N at an angle 45°	30
Fig. 4.17	Screenshot of total deformation of foot model by applying 700N at an angle 45°	30
Fig. 4.18	Screenshot of total deformation of foot model by applying 800N at an angle 45°	31
Fig. 4.19	Screenshot of Von-Mises stress of foot model by applying 600N at an angle 90°	31
Fig. 4.20	Screenshot of Von-Mises stress of foot model by applying 700N at an angle 90°	32
Fig. 4.21	Screenshot of Von-Mises stress of foot model by applying 800N at an angle 90°	32
Fig. 4.22	Screenshot of Von-Mises stress of foot model by applying 600N at an angle 120°	33
Fig. 4.23	Screenshot of Von-Mises stress of foot model by applying 700N at an angle 120°	33
Fig. 4.24	Screenshot of Von-Mises stress of foot model by applying 800N at an angle 120°	34
Fig. 4.25	Screenshot of Von-Mises stress of foot model by applying 600N at an angle 45°	34
Fig. 4.26	Screenshot of Von-Mises stress of foot model by applying 700N at an angle 45°	35
Fig. 4.27	Screenshot of Von-Mises stress of foot model by applying 800N at an angle 45°	35

LIST OF TABLES

PAGE NO

Table 1.1	Mechanical properties of bone	8
Table 4.1	Results of the maximum deformation and stress obtained for different values of forces acting on the same joint at three different angles.	36

ABSTRACT

In recent years, skeletal models of the human body are used to review biological structures and performances. The analysis of foot is of considerable interest, as it has physical interaction between the body and the surroundings throughout locomotion. Analysis will be vital for understanding the impact of mechanics during human standing and motion. It is difficult to directly measure the stresses on the foot. However, by using FEA, a 3D model of the foot is created from CT scan images and analyzed for stress and deformation using ANSYS. The distribution of stress within the foot model of human not only depends on the geometry but also on the structure and application of load on the foot. Using MIPAV software, a combined image was generated from CT scan segmented images. 3-D model of the human foot was developed using ITK SNAP software. The complete 3D model of foot was generated and imported into ANSYS and meshed. Static structural analysis (load & deformation) was carried out in ANSYS at different loading conditions. The deformation and stresses of the human foot were evaluated at various static loading conditions. The results were used to study the biomechanics/design of human foot during gait cycle.

Keywords: FEM, solid modeling, ANSYS, stress, deformation.

CHAPTER 1

INTRODUCTION

1. INTRODUCTION

Many studies on a foot joint skeletal model were done to evaluate stress using 2D or 3D finite element method (FEM). Stress distribution in the foot depends not only on the geometry but also on the structure of the model of foot. In order to provide a more realistic representation, it is necessary to develop a foot model in three dimensions. The 3D model of foot bone was shown in [Fig.1.1](#). Over the last decade the use of FEM as analysis tools in biomechanics and orthopedics has grown rapidly [1]. The purpose of this study was to analyze the state of finite element modeling of human foot using ANSYS software and to validate the stress and deformation. Finite element analysis (FEA) is composed of a computer model of a material/object used in designing a new product, and getting the product smoothness. There are basically two types of modeling: 2D and 3D modeling. Although, simplicity is given on 2-D modeling it tends to yield less accurate results. In 3-D modeling, more accurate results can be achieved, which requires high speed computers. Programmer can implant diverse functions or algorithms in each of these modeling schemes, which may accomplish if the system behaves non-linearly or linearly [1].

The key to understanding the function during various gait analysis is the stress within and between different structural foot elements. The FE model has the capability to acquire the data characterizing internal stress states and their evolution within bony structures under different static and dynamic loading scenarios. Based on basis of assumptions of simple geometry, limited relative joint movement, ignorance of certain ligaments structures and simplified material properties and the effect between the bones of foot, a number of foot models have been developed. Many researchers have focused on FE studies on the biomechanics of foot and analyzed under static loading conditions and focused on injuries of stress which are the most common foot injuries in athletes and military recruits [2]. Linear systems are limited composite and generally do not take into account deformation of plastic. Plastic deformation will be accounted for non-linear systems [3].

1.1 3D MODELING

The computer aided design (CAD) used to create a virtual three dimension object is known as 3D modeling. The process of developing a mathematical representation of any 3D

surface of object through software is called a 3D model. It can be displayed as a 2D image through a process called 3D rendering. Using 3D printing devices the model can also be physically created.

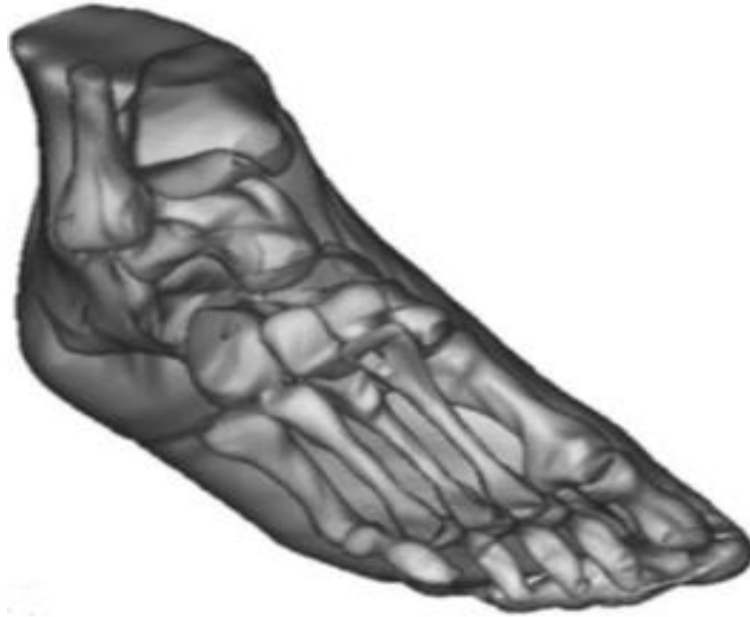


Fig. 1.1 Human foot bone model [4]

1.2 FINITE ELEMENT ANALYSIS

FEA models can be a very powerful method to understand the foot mechanical behavior [5]. Finite Element Analysis is a method in which a computational software is used to divide a solid model of a physical entity (the human foot in this case), into a large number of finite elements which are then solved to find out resultant parameters (stress, strain, deformation, etc.) when an input (load acting at a point) is given to the model. In case of structural failure, FEA may be used to help determine the design modifications to meet the new conditions [6]. There are basically three types of elements such as 1-D, 2-D and 3-D is shown in [Fig. 1.3](#).

There are particularly two types of analysis that are used in industry: 2D modeling and 3D modeling. Designing models in engineering practice presented numerous complex problems and challenges which can be easily addressed by FEA methods, which otherwise would have taken longer time. FEA provides a cost-effective and faster approach. It can determine the

suitability, sustainability and efficiency of prototypes prior to physical manufacturing and testing. FEA is proving especially useful in biomechanical simulations where CT scan data of a physical part can be used to generate a 3D solid model, which in turn can be divided/meshed using ANSYS and FE analysis can be performed[7]. For analyzing any physical system through computational method was shown in Fig.1.2.

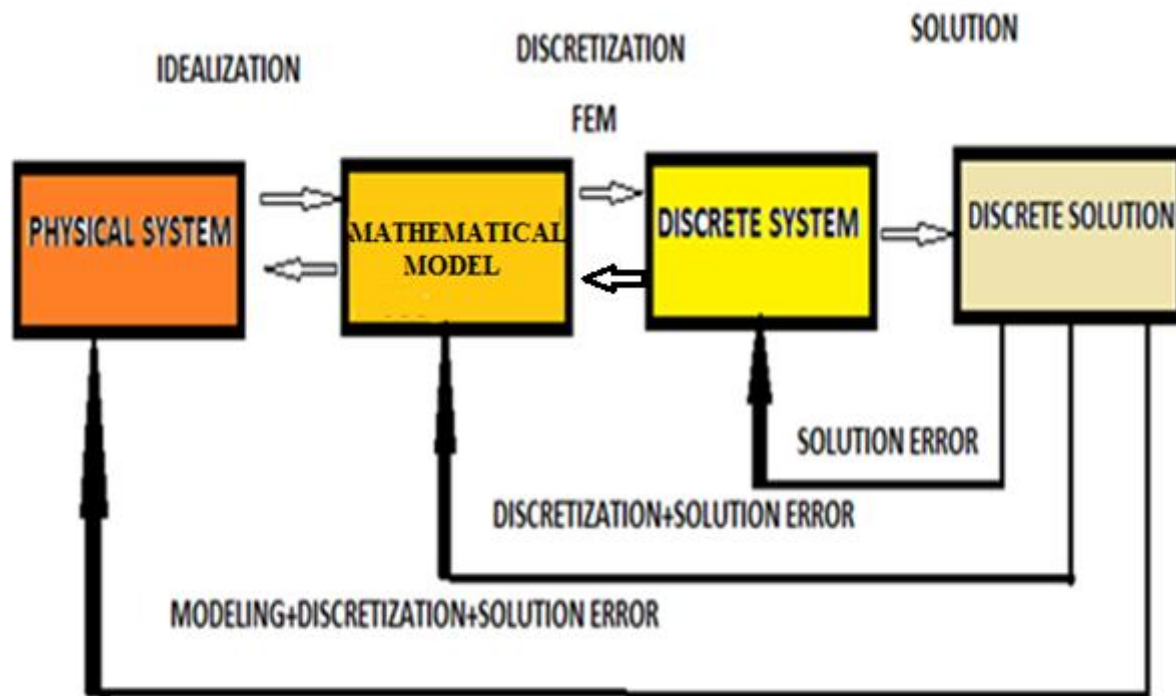


Fig. 1.2 Computational methods to analyse the physical system

FEA has become valuable and the basis of a multibillion industry in recent days. Numerical/mathematical solutions to even very complicated stress problems can now be obtained regularly by using finite element analysis. The most important function of mathematical modeling is that users of finite element codes should plan their strategy toward this end, supplementing the computer simulation with as much closed-form and experimental analysis as possible. Less complexity will be found in Finite element codes than many of the word processing and spread sheet packages found on modern microcomputers. FEA generally consists of three steps [9]:

- Preprocessing,
- Analysis and
- Post processing

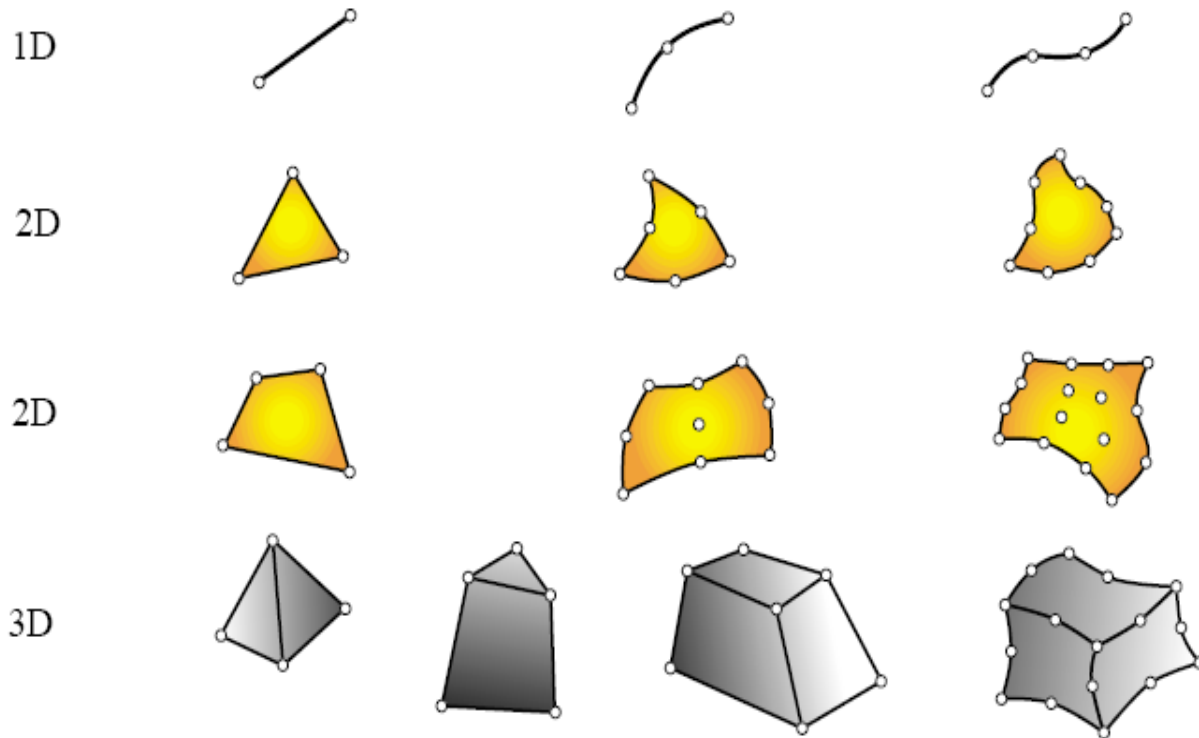


Fig. 1.3 Different element types [8]

1.3 BIOMECHANICS OF FOOT

Foot is the lowest part of the human leg. The body's natural balance-keeping system, makes humans capable of not only walking, but also running, climbing, and countless other activities only due to the foot's shape. The complex structure of foot contains ligaments, muscles that move nearly the joints while bones provide structure and more than 100 tendons. The structure of the hand is similar to that of the foot. Although, foot is less mobile it carries more weight and is stronger than the hand. The largest bone of the foot, the calcaneus, is commonly referred to as the heel of the foot. It slopes upward to meet the tarsal bones, which point downward along with the remaining bones of the feet. It is a viscoelastic material. Elastic

material properties are used for the cortical shell and for the cancellous bone in most FEM of joints.

1.4 ANATOMY AND BIOMECHANICS OF THE FOOT

The human foot is a very complex structure [10]. Part of the lower extremity, the foot, consists of 28 bones: 7 tarsal bones (talus, calcaneus, navicular, cuboid, medial, intermediate, and lateral cuneiforms), 5 metatarsal bones, 14 phalanges (two phalanges of the great toe, the other toes each three phalanges) and 2 sesamoid bones at the first metatarsophalangeal joint. The skeletal framework of the foot is divided into the tarsus (seven irregular bones), which is often subdivided into mid-foot (navicular, cuboid, and the three cuneiforms) and hindfoot (calcaneus and talus). A total of 13 tendons crosses the ankle joint (extrinsic muscles) and inserts at a bone of the foot. Many more intrinsic muscles originate and insert within the foot itself. Over 100 ligaments and 19 muscles are described in the foot and ankle, where they act as static stabilizers of the complex interplay of all the foot and ankle joints [11]. The total anatomy of foot was shown in [Fig.1.4](#). The material properties used for bone material are tabulated in [Table1.1](#).

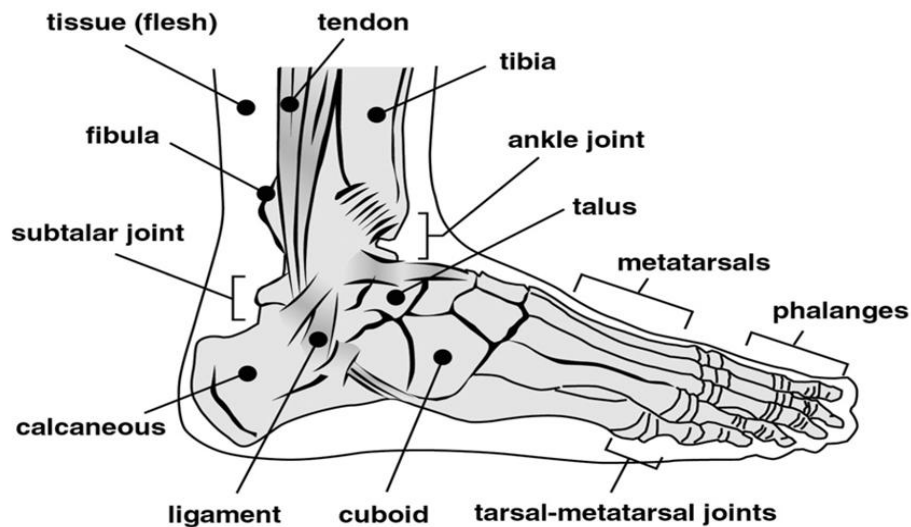


Fig. 1.4 Anatomy of foot [12]

Table 1.1 Mechanical properties of bone.

Bone type	Young's modulus [MPa]	Poisson's ratio(ν)	Density [kg/m^3]	UTS [MPa]
Cortical	$17 \times 10^3 - 19 \times 10^3$	0.25	2000	150
Cancellous	100-200	0.30	1500	20

Fig. 1.5 shows the heel-strike of foot during normal walking. In the first step heel strikes the ground. In the second step the mid-foot makes contact and in the third step forefoot remains in contact. Majority of runners have encountered in the clinic run, a rear foot striking pattern during which initial contact occurs at the heel. These individuals also tend to demonstrate longer strides, decreased stride rates, and experience greater impact peaks of ground reaction forces (GRF) at initial contact. Research has shown that power absorption of the lower extremity in these runners occurs primarily at the knee [13]. These individuals will commonly experience anterior knee pain, tibial stress fractures, lower back pain, and plantar fasciitis. With the recent emergence of the “barefoot running craze”, there is an increasing number of individuals who demonstrate a forefoot striking pattern. Runners with this type of style demonstrate initial contact closer to the lateral ball of their foot, shorter stride lengths, increased stride rates, and experience less impact peaks of GRF. These individuals typically present with Achilles tendonitis, calf strains, metatarsal stress fracture, and foot pain [13]. Angle variation of different foot strike pattern was shown in Fig.1.6.

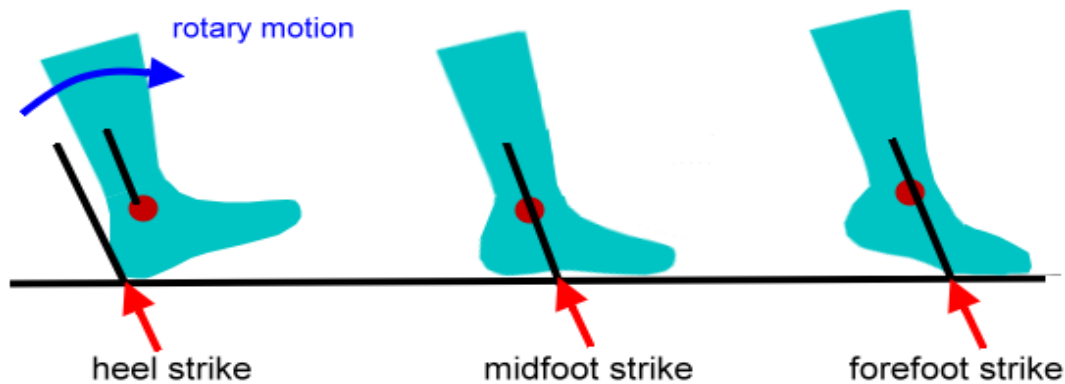


Fig. 1.5 Different foot strike patterns [14]



Fig. 1.6 Angle varies between different foot strike patterns

In Fig.1.7 the line of gravity and contact point of the foot was shown in standing condition. Here the contact point was in the middle of the foot. The center of gravity varies according to the position and orientation of foot. The three planes of foot, frontal plane, sagittal plane and the transverse plane was shown in Fig. 1.8. The frontal plane passes through the ankle joint and is parallel to the media-lateral direction. The sagittal plane passes through the ankle joint and is parallel to the longitudinal plane of the body. The transverse plane is parallel to the ground. The sequence of segmented CT images of the foot obtained is shown in Fig. 1.9 below. From the processed CT images the foot model was reconstructed with the use of various segmentation techniques.

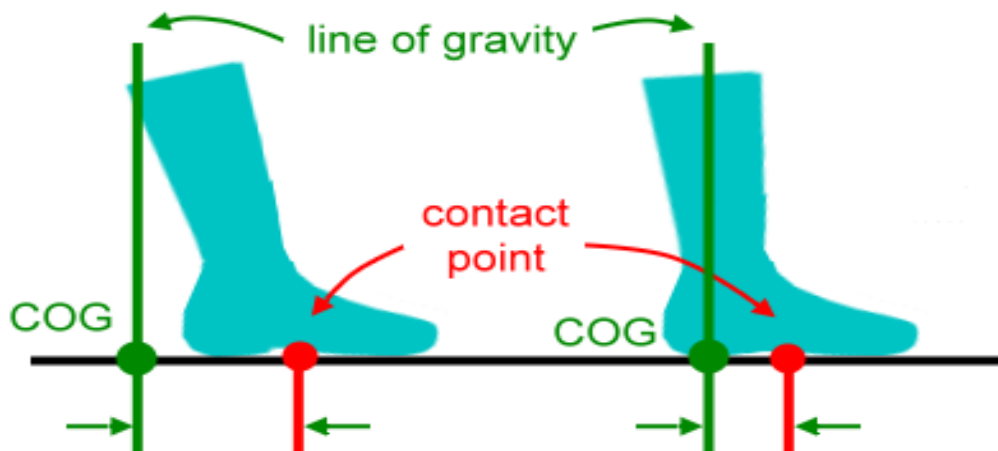


Fig. 1.7 Foot strike close to COG[13]

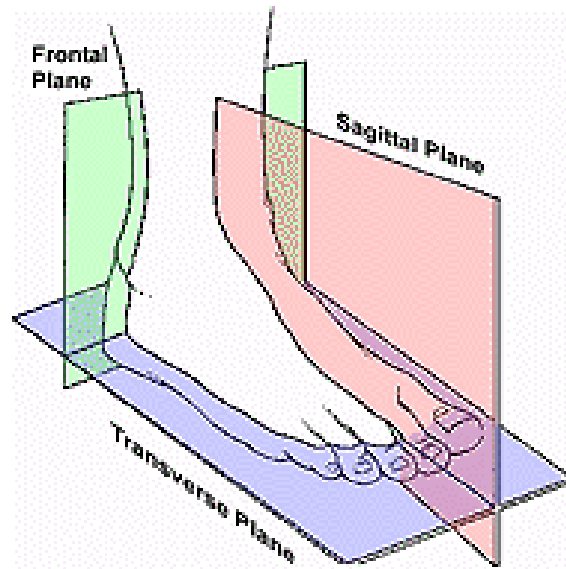


Fig. 1.8 Three types of plane of foot [14]

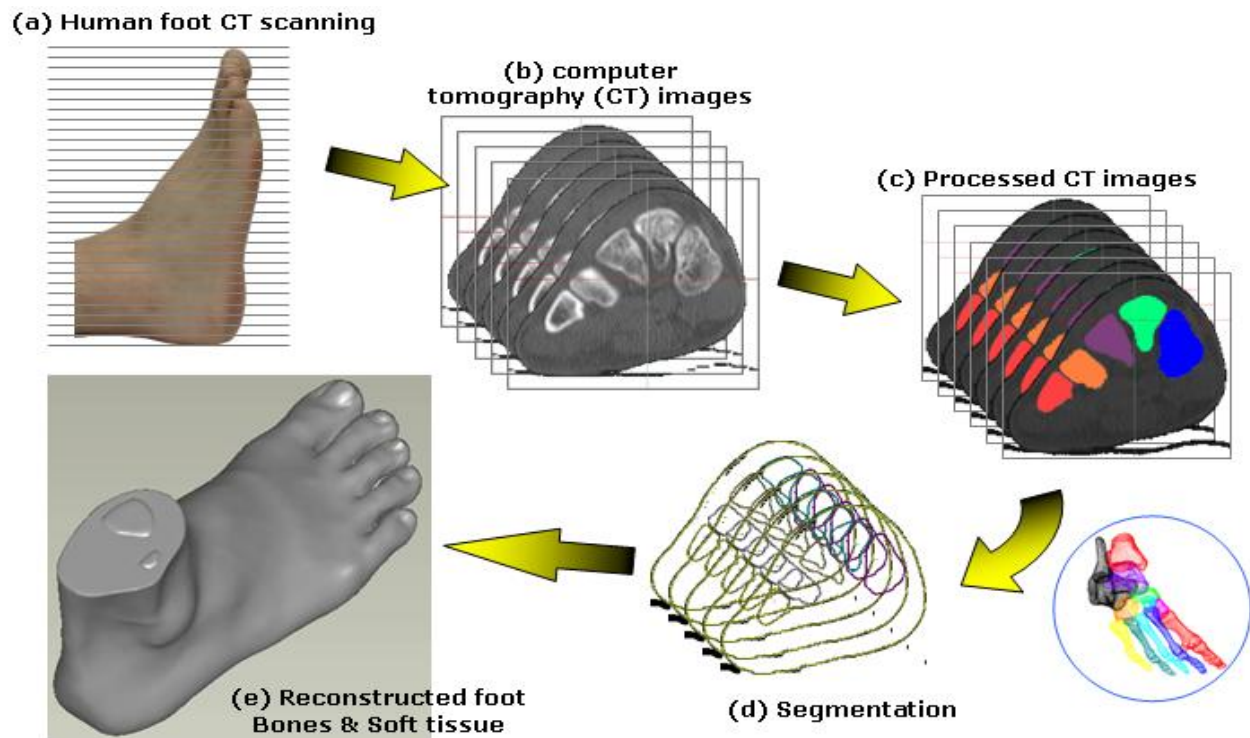


Fig. 1.9 Segmentation of a human foot from individual coronal CT slices [19]

CHAPTER 2

LITERATURE REVIEW

2 INTRODUCTION

In this project a 3D model of foot was created from 2D images of foot. Then the model was imported to ANSYS for various analysis. Various types of analysis such as total deformation and stress was done in static structural of ANSYS by applying various forces such as 600N, 700N, 800N at different angles.

2.1 3D MODELLING

3 Types of 3D Computer Models

Wireframe

Surface Model

Solid Model

The wireframe model is built up using a series of connected lines to produce a 3D object. The surface model is built up by drawing the surfaces of an object. Like adding the canvas onto the frame of a tent. The solid model is built up by using simple geometric forms or extrusions - such as cuboids, cylinders & prisms. These can be added or subtracted to produce complex 3D models was shown in [Fig. 2.1](#).

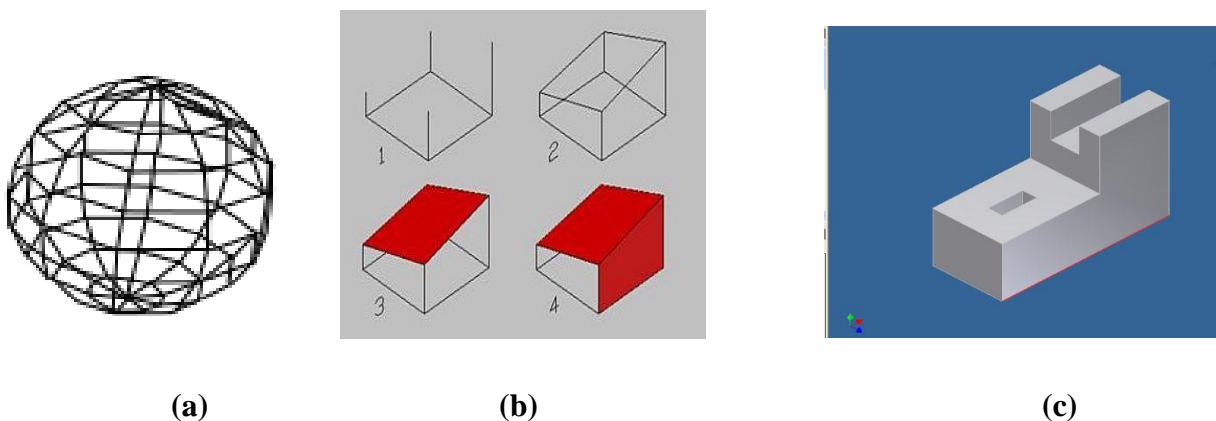


Fig. 2.1(a) Wireframemodel, (b) Surface model and (c) Solid model

Different mathematical tools have been developed in recent years to address the common quandary encountered by physicians when assessing fracture risk prediction in patients found to

have a metastatic bone lesion. Therapeutic approach is one of the methods which consider bone as a structure, whose mechanical behavior depends on both material and geometric properties [15].

Computer models provide several benefits than other types of models (such as foot casting). For example, a number of computer models can be developed and tested in different conditions but the primary characteristic of the model is maintained after exhaustive testing. Computer models also provide information which cannot be easily obtained over other types of models, such as load distributions within soft tissues, internal stresses, joint reaction forces, and muscle force analysis. Simulations can be performed quickly and at low cost in diverse situations including injury, surgery, dynamic motion simulation, and graphical animation of the experiment by developing the accurate computer model. Also models help to determine the underlying mechanisms. The FE model has capability to predict the internal stress within the bone which makes it a valuable tool in the study of ankle-foot complex in biomechanics. An overall stress distribution of the foot can be predicted by computational analysis of foot in biomechanics. Computer models not only require a detailed representation of foot geometry and joint characteristics, but also require realistic loading conditions to depict the internal stress and strain distributions in the model of foot complex [16].

These geometries were used to create a 3-D anatomically detailed foot model that will serve as the basis for a finite element foot model. One important consideration was the amount of load applied to the foot while it was scanned. Because computer simulations typically start with unloaded initial conditions, scanning a minimally loaded specimen might be ideal for generating anatomical data for finite element modeling [17].

A wide variety of insole geometries, structure and materials can be tested within the future so as to check and improve the foot comfort through the modification of insole geometrical style/design and/or insole materials of formulation. Because of the difficulties in understanding the biomechanics of the complicated human foot and ankle structures from experimental studies alone, computational model is needed to provide a viable alternative to predict their biomechanical behavior [18].

2.2 FINITE ELEMENT MODEL OF FOOT-ANKLE COMPLEX

The FEM is a versatile numerical method which allows stress and strain analyses of complex structures with irregular geometry and material nonlinearities. When a foot structure is loaded, stresses are generated in different materials (i.e. tissues). The distribution of these stresses, their magnitudes and orientations throughout the structure, is a result of complex interplay of the foot skeleton, cartilages, muscles, ligaments, fascia, and the external environment that arises from foot and ground interactions. In such a model that mimics the real structures to a certain degree of refinement, the structural aspects (geometry, material properties, and loading/boundary conditions) are required to be expressed mathematically [19].

In using the FEM, the model of the human foot as a geometrical entity, has to be first defined. Modern musculoskeletal imaging techniques such as magnetic resonance imaging (MRI) and computer tomography (CT) can be a source for such complete anatomical structures. The geometrically complex foot structures, are then discretized into finite number of relatively simple elements (i.e. FE mesh generation), connected by nodal points or nodes. Each element can have its own material properties. The equations for describing the mechanical behavior of these elements are known. The computer program (e.g. ABAQUS, ANSYS) can calculate the stiffness matrix of each element, and the stiffness matrix of the whole structure is determined. Knowledge of the structural stiffness matrix, of the loads and the boundary conditions allows the response of a model to any form of external loading to be predicted [19].

2.3 OBJECTIVE

The objective of this study is to evolve a comprehensive FE model of the foot using 3D geometry of skeletal components of the bony structures of foot and to evaluate the deformation, stress and strain acting on a 3D model of the human foot using ANSYS software. The purpose of this study was the development of a foot joint skeletal model using the finite element method for the analysis of physical exercise, sports injury and footwear design.

CHAPTER 3

METHODOLOGY

3 METHODS

The softwares used in this experiment are:

- MIPAV
- ITK SNAP
- MESHLAB
- SOLID WORKS
- ANSYS

This study built up the model using CT data. The database maintained includes complete CT images of the whole human body in slices. The basic methodology for retrieval of anatomical structures was outlined in the shows the modeling process of the hard bones of the foot and ankle. The 2D CT slices images were converted into 1 combined image using the MIPAV software. The combine 2D CT image was converted to a 3D image using ITK snap which is capable of handling CT data. Then the 3D image was cleaned. Then it was converted into ANSYS file format (.IGS) in the next step, followed by volume generation and importing to ANSYS (ANSYS, Inc., Canonsburg, USA) for meshing the model. Thus, the FE model of bony structures was developed. The models of foot were individually constructed, because the CT data of foot was available in single files. They were combined using ANSYS. After then analysis was done by using ANSYS software. The method was shown in [Fig.3.1](#).

The following methods are involved

- Combining the sequence image into 1 image.
- 3D reconstruction of model
- Cleaning of the model.
- Convert the model into ANSYS file format.
- Meshing.
- Analysis and Finite element results.

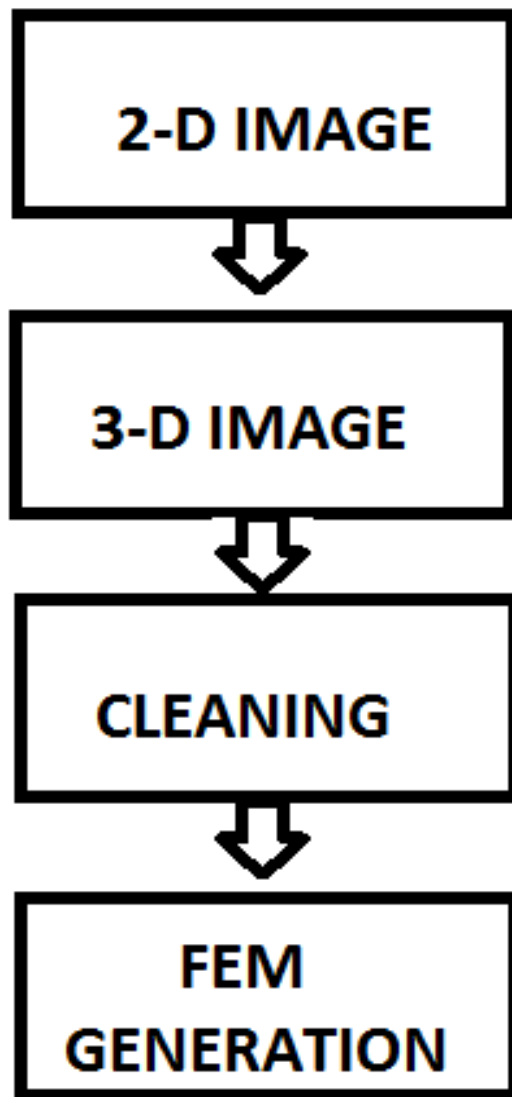


Fig. 3.1 Schematic diagram showing the FEM generation

3.1 COMBINING THE CT SCAN IMAGE SEQUENCE

The geometry/algebra of the FE model was obtained from 3D reconstruction of CT images from the right and left foot of a healthy male subject of age 30, height 160 cm and weight 60 kg. Coronal 174 CT images were taken with intervals of 0.7227mm in the neutral unloaded position. This can be achieved by MIPAV (Medical Image Processing and Visualization) software. In this software sequence images can be converted into one combined image.

3.2 3D RECONSTRUCTION

The 3-D image was constructed from 2D image of human foot using ITK SNAP. ITK-SNAP is an interactive application software that allows users to navigate three-dimensional medical images, manually delineate anatomical regions of interest, and perform automatic image segmentation. ITK-SNAP is most frequently used to work with magnetic resonance imaging (MRI) and computed tomography (CT) data sets.

ITK-SNAP is open source software distributed under the GNU General Public License. It is written in C++ and it leverages the Insight Segmentation and Registration Toolkit (ITK) library. ITK-SNAP can read and write a variety of medical image formats, including DICOM, NIFTI, and Mayo Analyze. It also offers limited support for multi-component (e.g., diffusion tensor imaging) and multi-variety imaging data.

3.3 CLEANING OF THE MODEL

After the 3-D image was constructed, it was inserted into MESHLAB for Cleaning, repairing, smoothing and size reducing of the 3D model. There are many types of smoothing such as LAPLACIAN smooth, TAUBAIN smooth, GAUSHIAN smooth, HC LAPLACIAN smooth. Unsharp mask geometry is an option in which the sharp object can be removed. By using ‘remove duplicate face’ it will remove any duplicate faces present in the model. By using ‘remove zero face’ it will remove the zero area face.

MESHLAB is used for the cleaning of the surface without distorting the shape. The general working principle behind the software is that it allows the nodes present in the elements to come closer leading to reduction of any sharp edges in the model.

3.4 CONVERTING INTO ANSYS FILE FORMAT

In order to work with ANSYS, first the foot model should be imported into ANSYS. So that the foot model should be converted into a suitable importing format for ANSYS. There are many types of importing format of ANSYS such as .AQDB, .DB, .CFX, .XML, .BGD, .IGS, .SAT,

.DWG. Another software tool, SOLIDWORKS was used to convert the .STL file into .IGS format.

3.5 IMPORTING THE MODEL INTO ANSYS

After converting the foot model in solid works the model was imported into ANSYS for observation and analysis.

3.6 MESHING

Trigonal meshing was obtained in this model. The solid model which was obtained in previous was then imported into ANSYS. The internal communication between the cuneiforms, cuboid, calcaneus, navicular, talus, tibia, fibula, metatarsals and all others were connected before meshing. After meshing simulation of the interaction between the joint surfaces, was done by ANSYS.

3.7 ANALYSIS – DEFORMATION

Analysis was done in ANSYS After meshing. Various types of analysis was done by applying load to the model. Post-processing tools for ANSYS Fluent can be used to generate meaningful graphics, animations and reports that make it easy to convey fluid dynamics results. Shaded and transparent surfaces, pathlines, vector plots, contour plots, custom field variable definition and scene construction are just some of the post-processing features that are available. Solution data can be exported to ANSYS CFD-Post, third-party graphics packages or CAE packages for additional analysis. Within the ANSYS Workbench environment, ANSYS Fluent solution data can be mapped to ANSYS simulation surfaces for use as thermal or pressure loads. In standalone mode, ANSYS Fluent can map structural and thermal loads on surfaces and temperatures in volumes from ANSYS Fluent to third-party FEA meshes.

CHAPTER 4

RESULTS AND DISCUSSION

RESULTS AND DISCUSSION

The following results were obtained during this project. The 3D model of human foot bone was developed using various software tools. First the combined image was obtained from CT scan images. Then a 3D model was constructed from the 2D image. Then it was cleaned. After cleaning it was imported into ANSYS for analysis. Fig. 4.1 shows the step by step results of the current project.

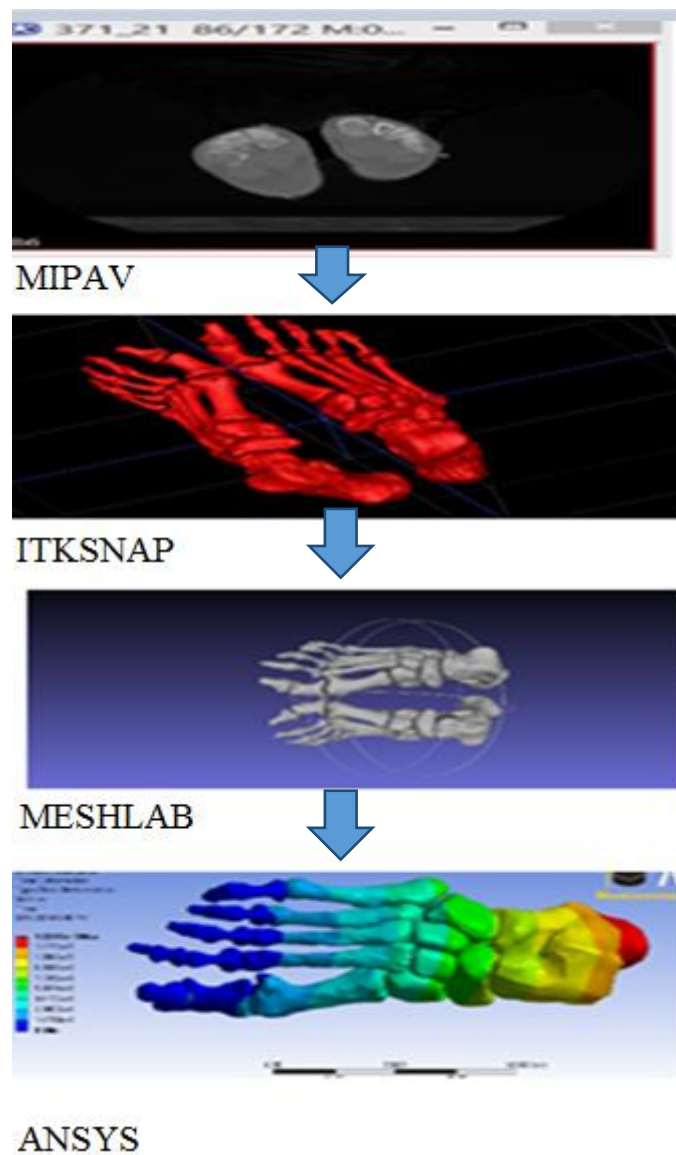


Fig. 4.1 Results of the Snap shots of various softwares

4.1 CT SCAN IMAGE SEQUENCE

One combining image was constructed from segmented images was shown in [Fig.4.2](#). The total 174 grey scale images were combined into one image in MIPAV software.

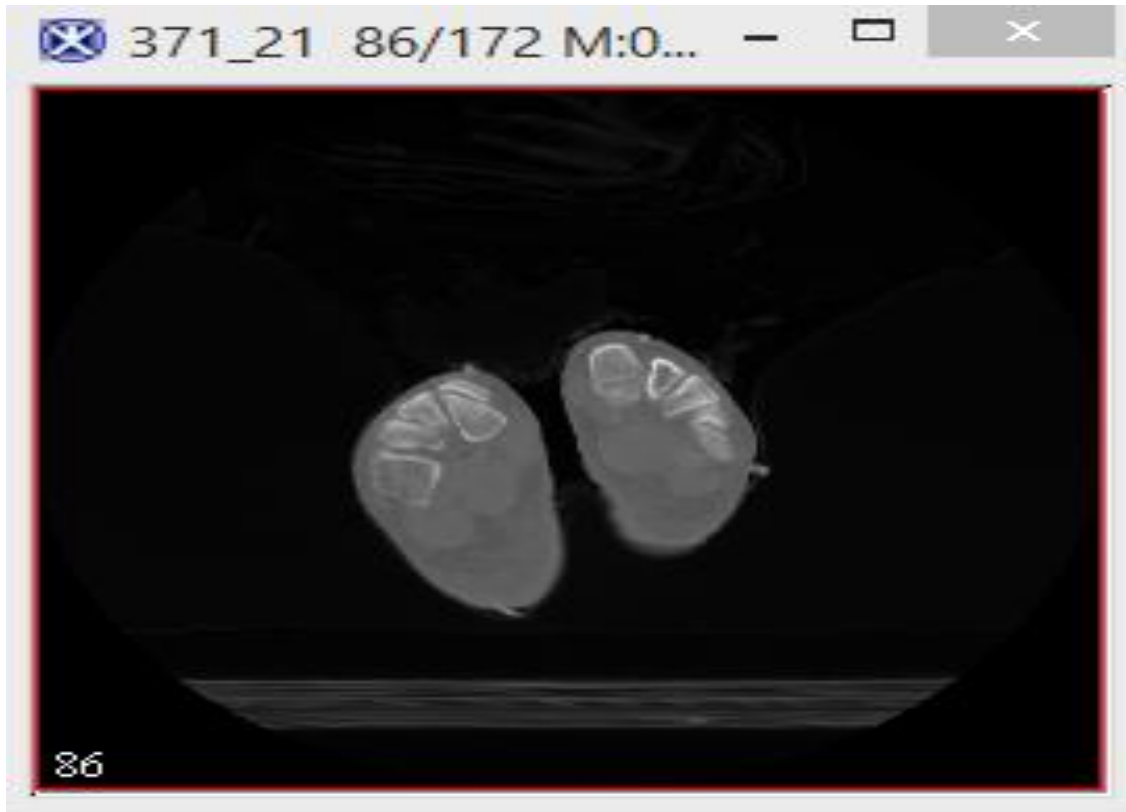


Fig. 4.2 Combined CT scan images using MIPAV

4.2 3D IMAGE CONSTRUCTED

3D image was constructed from the 2D image of CT scan image by using ITK SNAP software. [Fig. 4.3](#) gives the details of the grayscale image output. The total size of the image was 89088 Kb. The spacing of the segmented images is 0.7227mm. The byte order was found to be Big Endian. The orientation was found to be RIP. The three view such as: top view, side view and bottom view of foot model was shown in the [Fig. 4.4](#) and the constructed 3D model was shown in [Fig. 4.5](#).

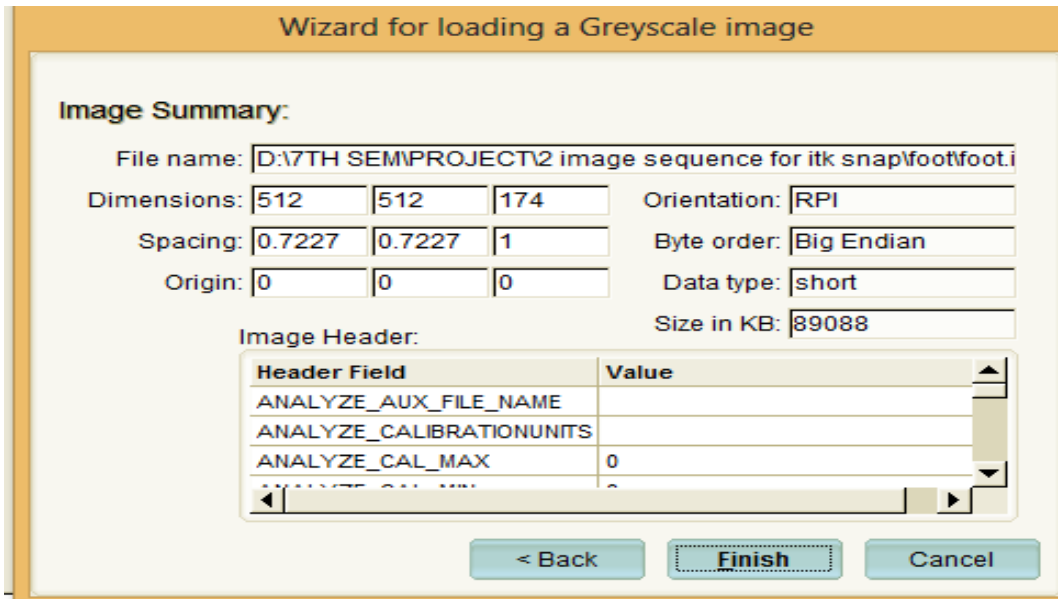


Fig. 4.3 The details of the greyscale image

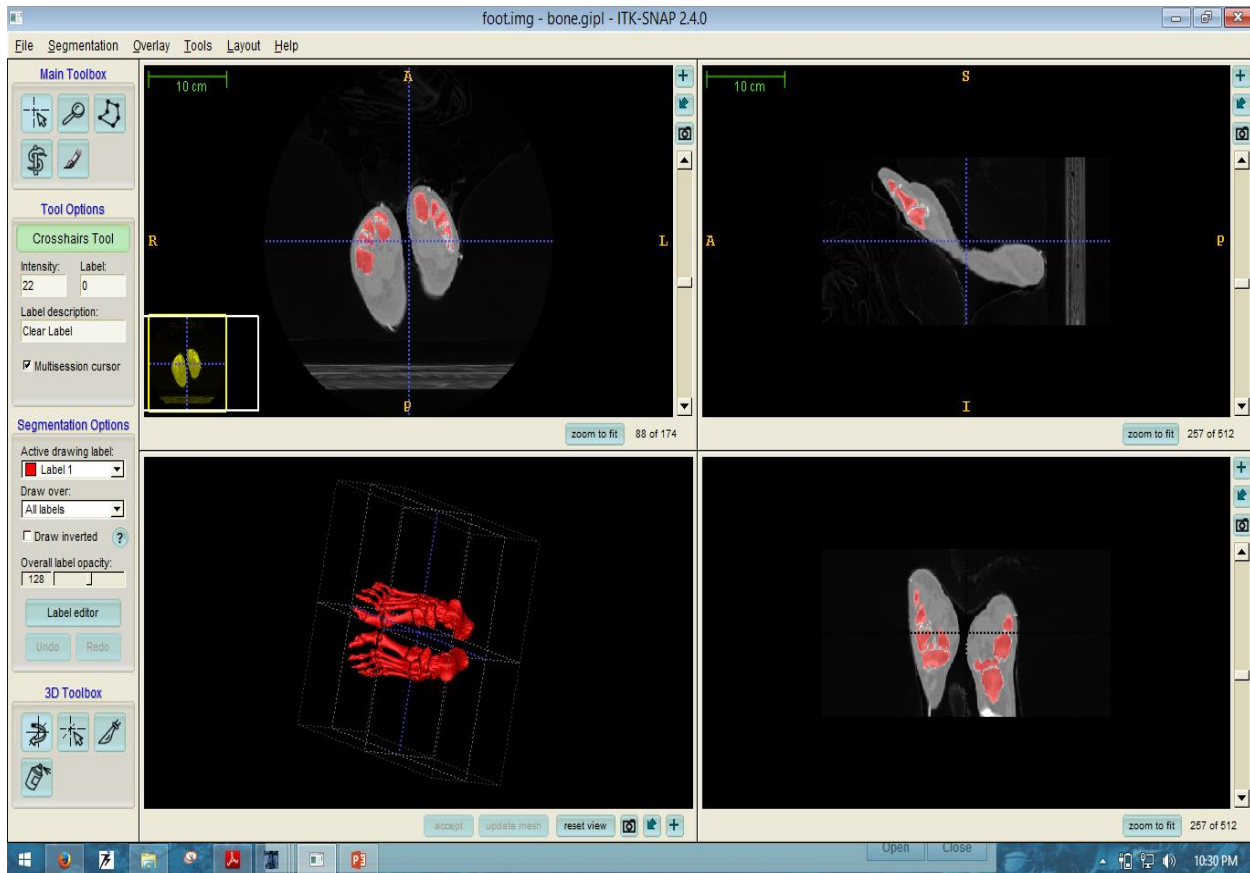


Fig. 4.4 Three-sectional view of model in ITKSNAP

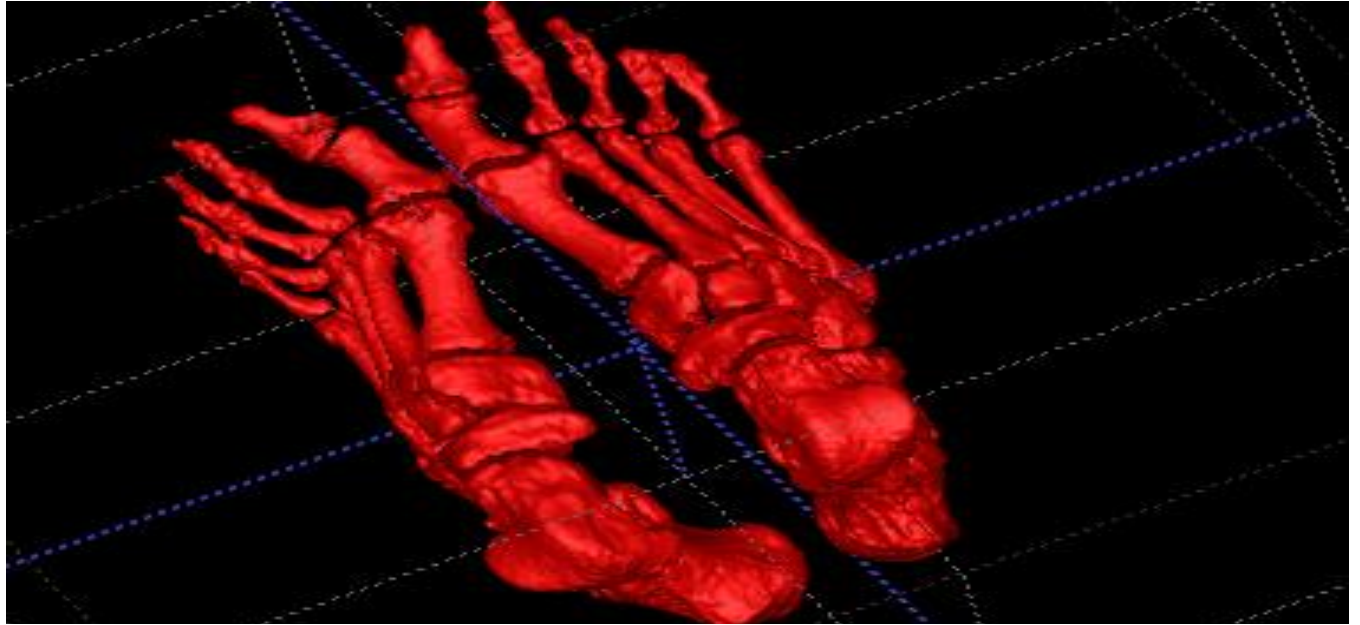


Fig. 4.5 Constructed 3d model of human foot bone

4.3 CLEANING, REPAIRING, SIZE REDUCING AND SMOOTHING

After constructing the 3D model of foot, it was cleaned in mesh lab. The cleaned and final model of the foot was shown in [Fig. 4.6](#).

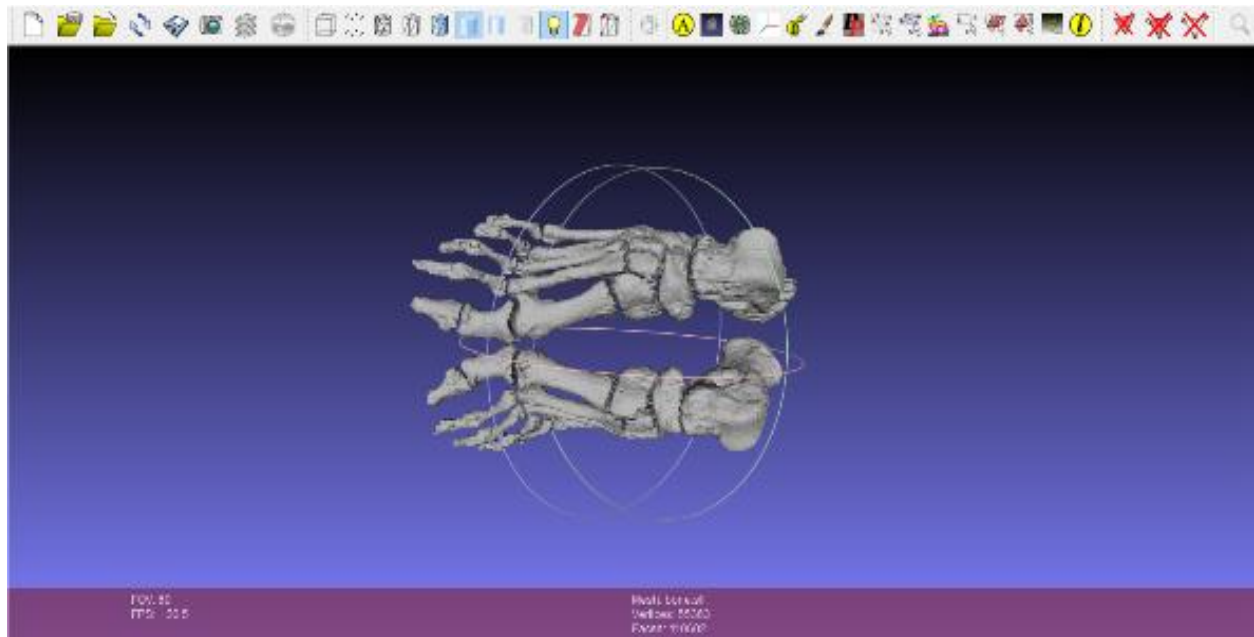


Fig. 4.6 Final model of foot after cleaning

After cleaning, the model was exported to .STL file format. The .STL file was converted to .IGS in solid works as shown in Fig. 4.7.

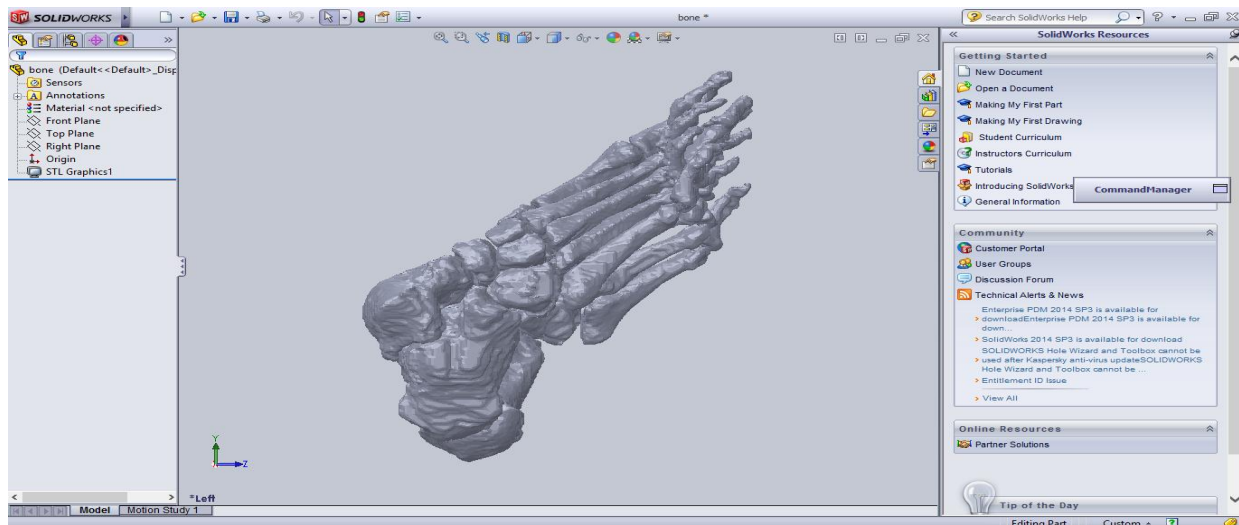


Fig. 4.7 Converting .STL to .IGS format for ANSYS in SOLID WORKS

4.4 ANSYS ANALYSIS

After constructed the final model in .IGS format, it is then imported into ANSYS for analysis as shown in Fig. 4.8. Triangular meshing was done as shown in Fig. 4.9.

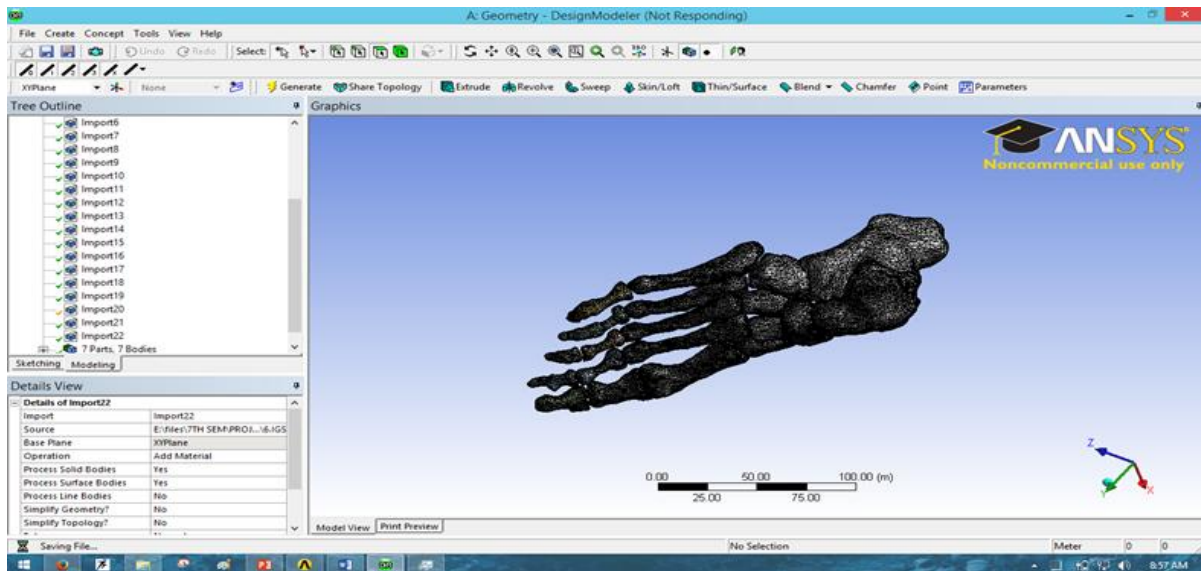


Fig. 4.8 Screenshot of model after import into ANSYS

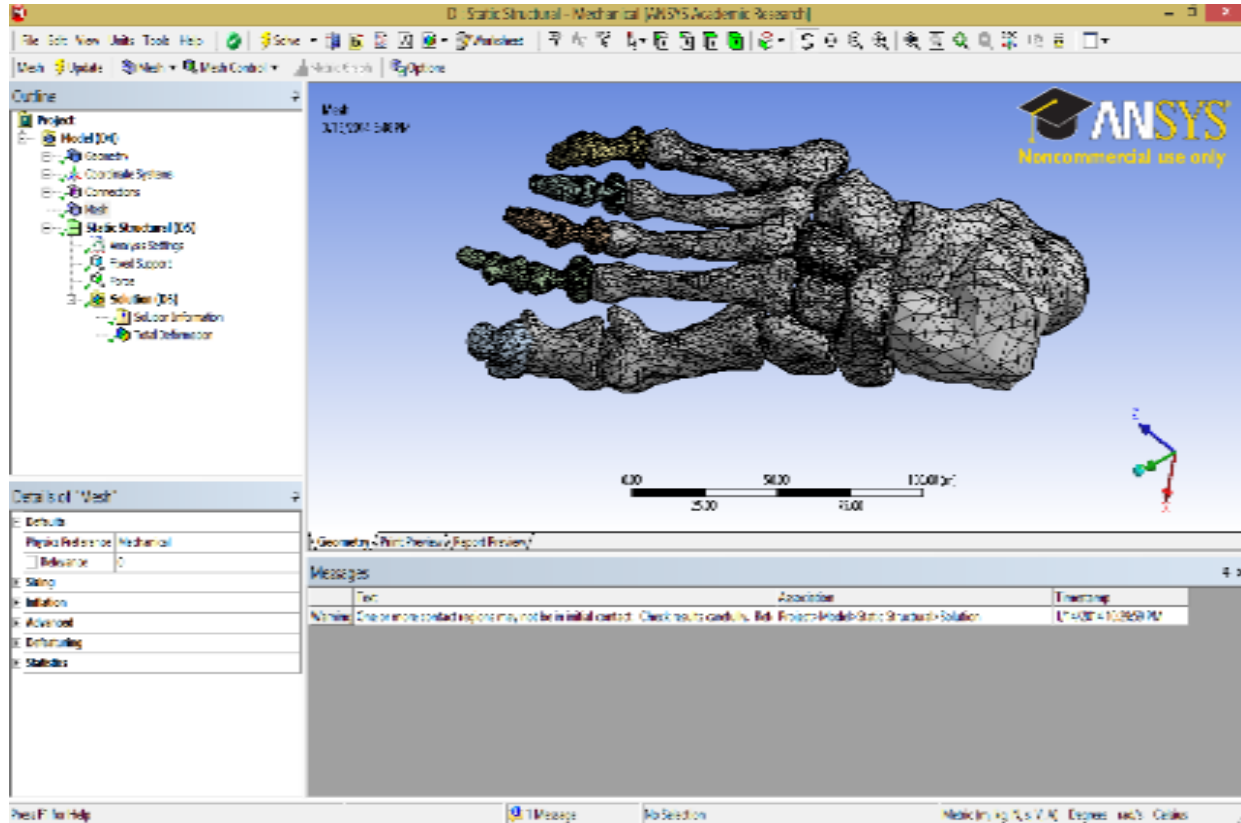


Fig. 4.9 Screen shot of mesh foot model in ANSYS

Boundary condition is applied to the meshed model and post processing is done. Various loads have been applied along different directions. Three different load angle was chosen (at an angle of 90° , 120° , 45°). The angle is so chosen as during normal walking on a flat surface, the load on the foot has an angle of 90° with the horizontal. During ascending or climbing a slope the load on the foot is assumed to have an angle of 45° . Similarly, while descending a slope the load on the foot is assumed to have an angle of 120° . Three different loads such as 600N, 700N and 800N was applied for each angle. At 90 degree the load was also applied in a direction normal to ground (horizontal). The total deformations of the model were calculated. The maximum total deformation was observed to be $7.948e^{-5}$ (.053553 m) and minimum was found to be 0 shown in Fig. 4.10.

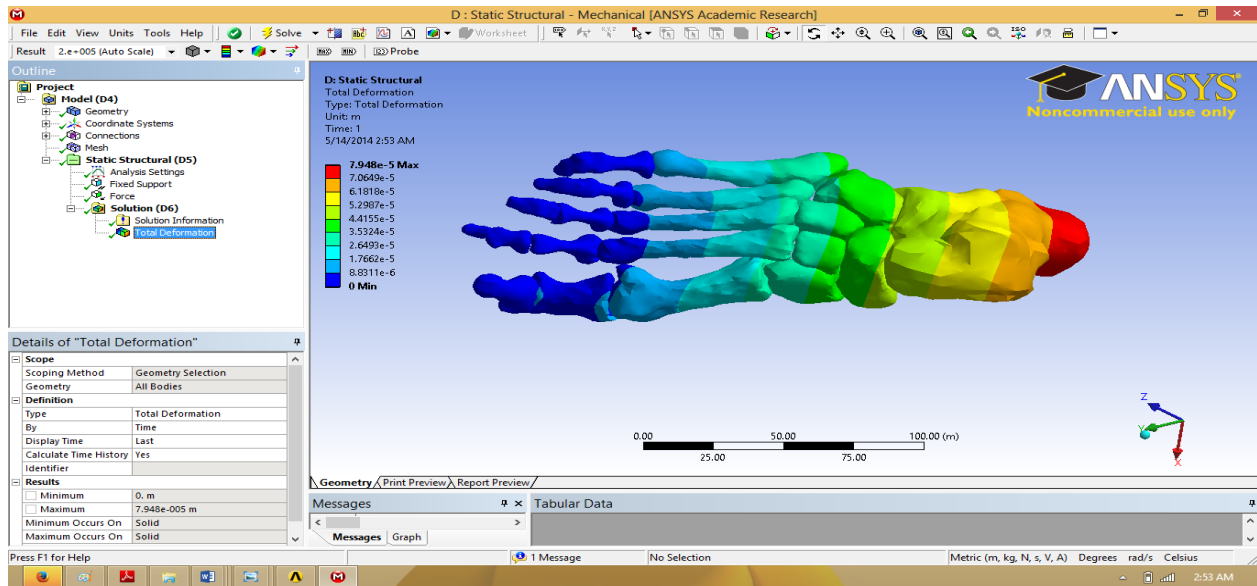


Fig. 4.10 Screenshot of total deformation of foot model by applying 600N at an angle of 90°

Secondly, 700N force was applied in a direction normal to ground. The maximum total deformation was observed and it was found to be 9.2726×10^{-5} (.062478m). The minimum deformation was found to be 0 as shown in Fig. 4.11.

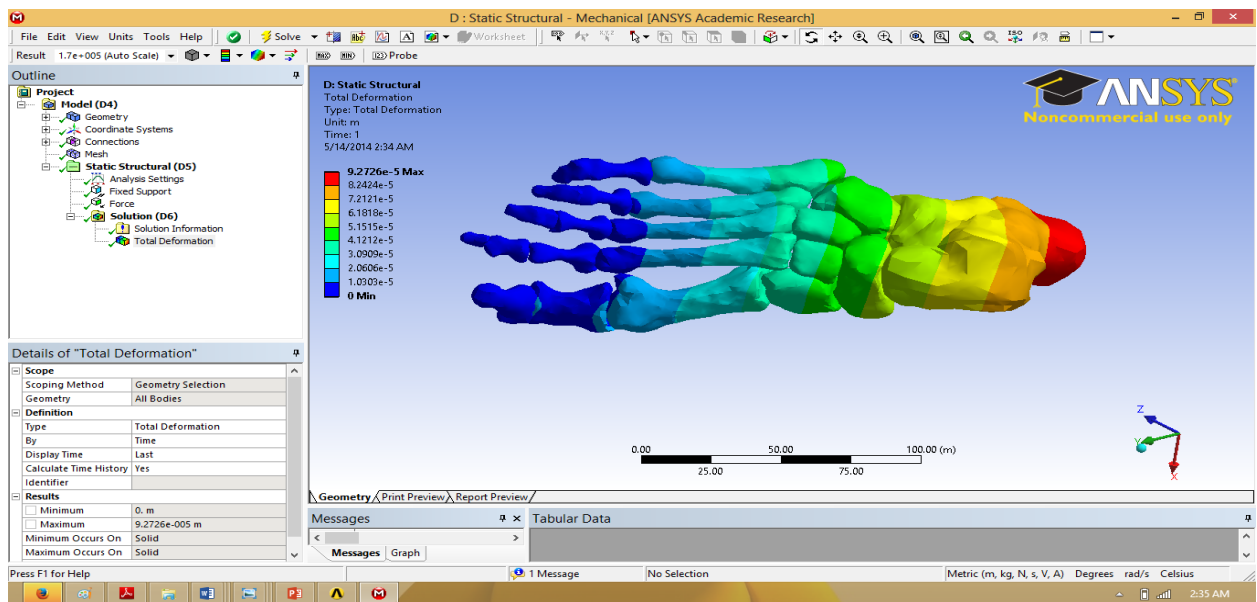


Fig. 4.11 Screenshot of total deformation of foot model by applying 700N at an angle of 90°

Finally, 800N force was applied normal towards the horizontal. The maximum total deformation was observed and it was found to be 9.935×10^{-5} (.066941m) and the minimum was found to be 0 as shown in Fig. 4.12.

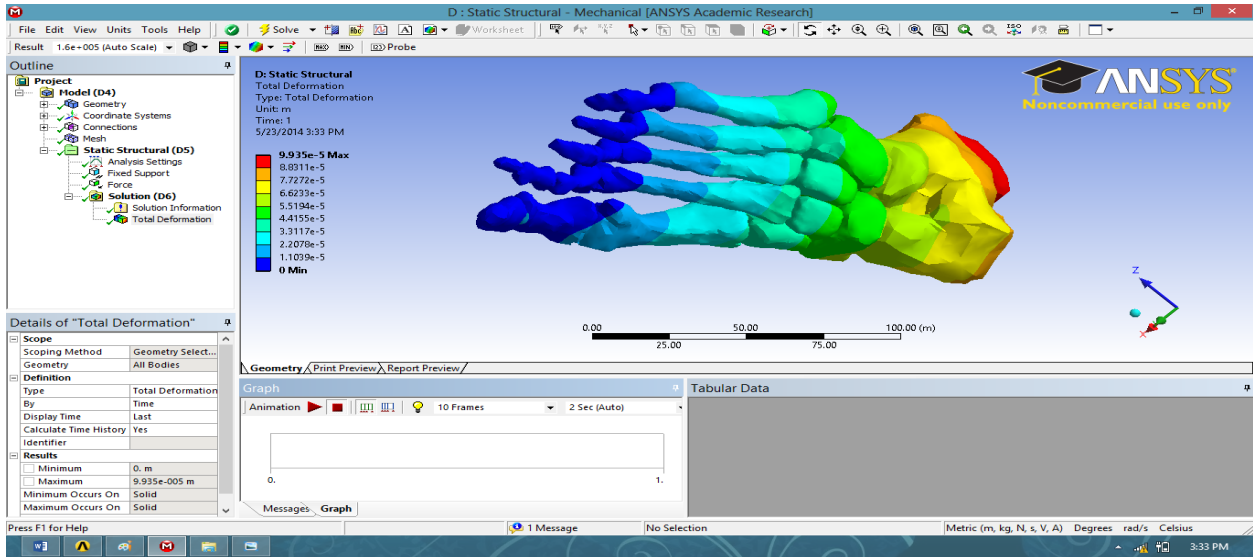


Fig. 4.12 Screenshot of total deformation of foot model by applying 800N at an angle of 90°

Then total deformation was calculated at 120° angle. First 600N was applied. The maximum deformation was found to be $3.83e^{-5}$ (0.025806 m) and the minimum deformation was 0 as shown in Fig. 4.13.

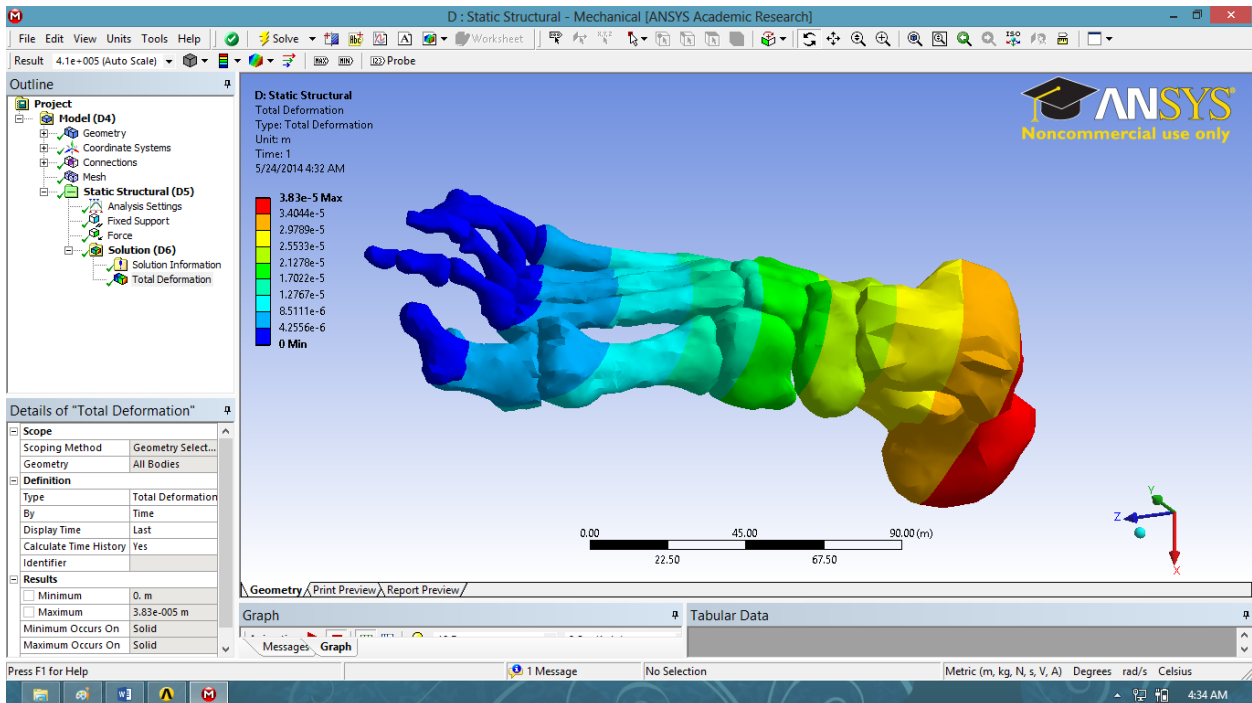


Fig. 4.13 Screenshot of total deformation of foot model by applying 600N at an angle 120°

By applying 700N, the maximum deformation was found to be $4.4683e^{-5}$ (0.030107 m) and minimum was 0 as shown in Fig. 4.14.

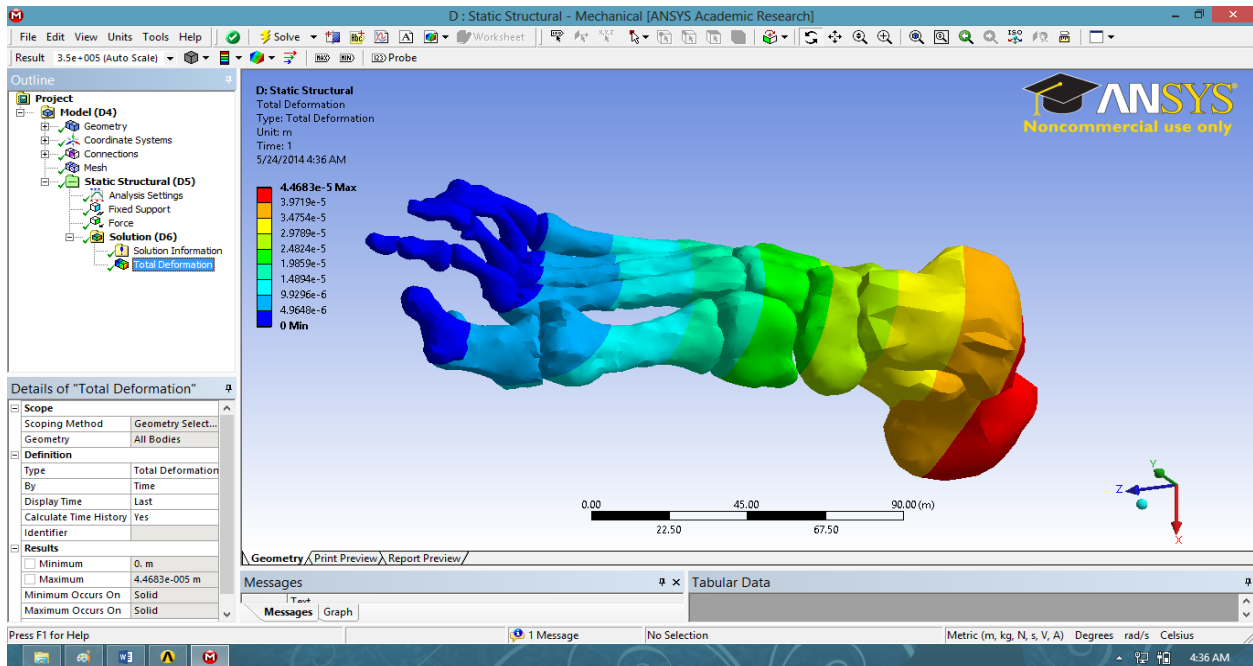


Fig. 4.14 Screenshot of total deformation of foot model by applying 700N at an angle 120°

By applying 800N maximum deformation was found to be 5.1067×10^{-5} (0.034408 m) and the minimum deformation was 0 as shown in Fig. 4.15.

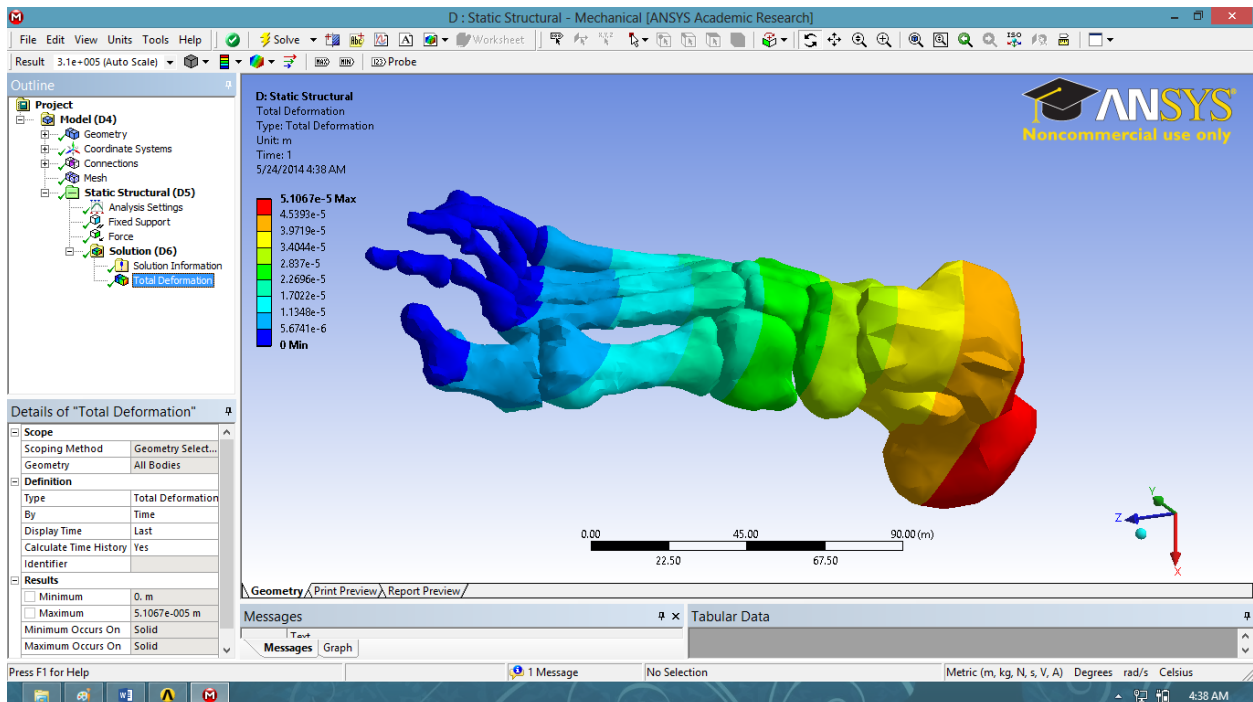


Fig. 4.15 Screenshot of total deformation of foot model by applying 800N at an angle 120°

Finally, the total deformation was calculated for 45° angles. The maximum deformation was found to be $5.8855e^{-5}$ (0.039656 m) by applying force of 600N as shown in Fig. 4.16.

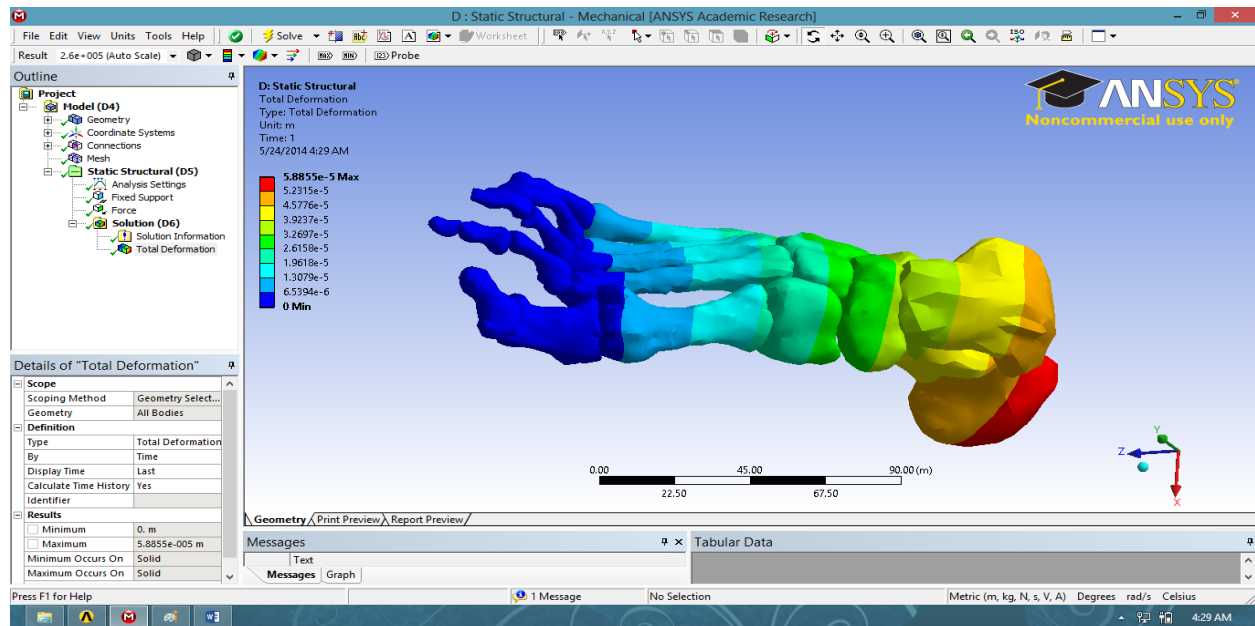


Fig. 4.16 Screenshot of total deformation of foot model by applying 600N at an angle 45°

By applying 700N, the maximum deformation was found to be $6.866e^{-5}$ (0.046262 m) and the minimum deformation was found to be 0 as shown in Fig. 4.17.

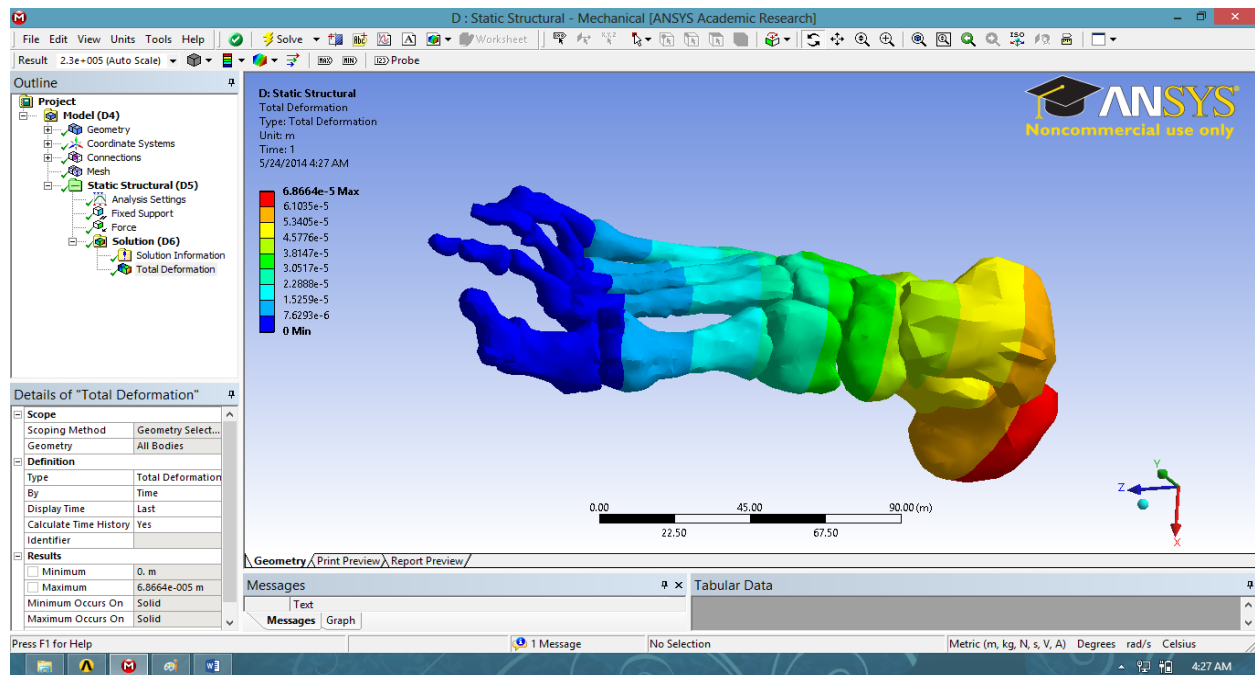


Fig. 4.17 Screenshot of total deformation of foot model by applying 700N at an angle 45°

By applying 800N, the maximum deformation was found to be $7.8473e^{-5}$ (0.052874 m) and the minimum deformation was found to be 0 as shown in Fig. 4.18.

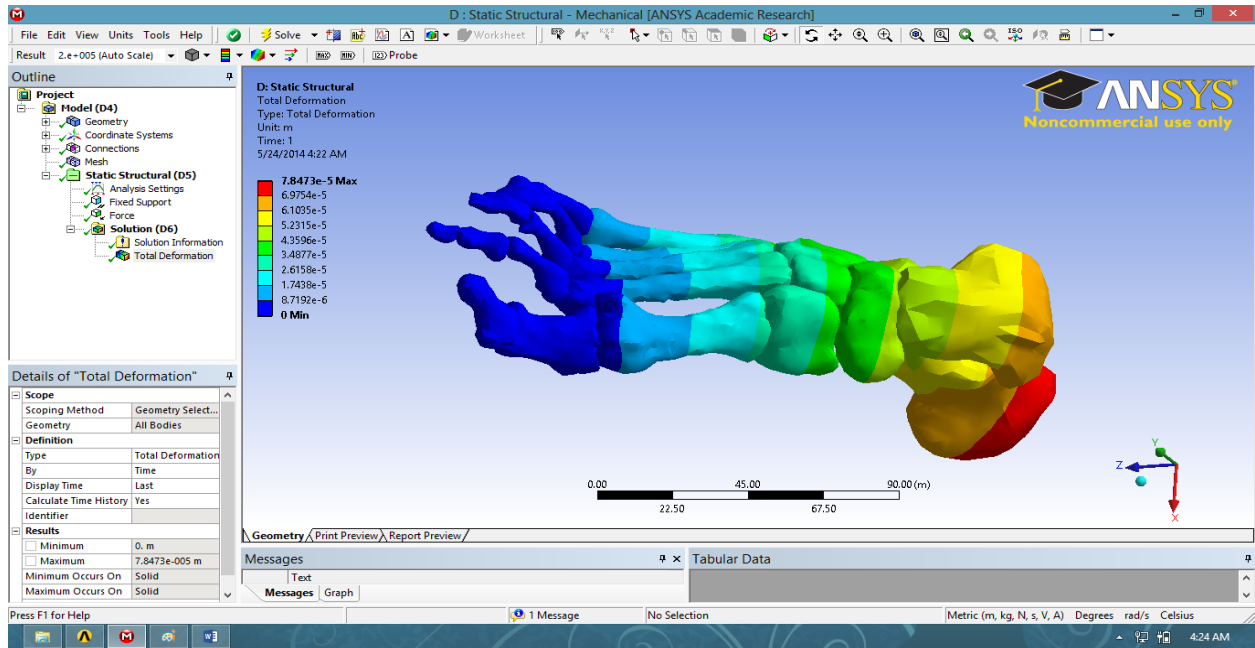


Fig. 4.18 Screenshot of total deformation of foot model by applying 800N at an angle 45°

Similarly Von-Mises stress was calculated by applying 600 N and 700N (Fig 4.19 and Fig 4.20 respectively) at an angle 90° . The maximum stress was found to be 978.66 Pa and 1141.8 Pa for 600 N and 700 N force respectively. In all the cases forces are applied normal to ground.

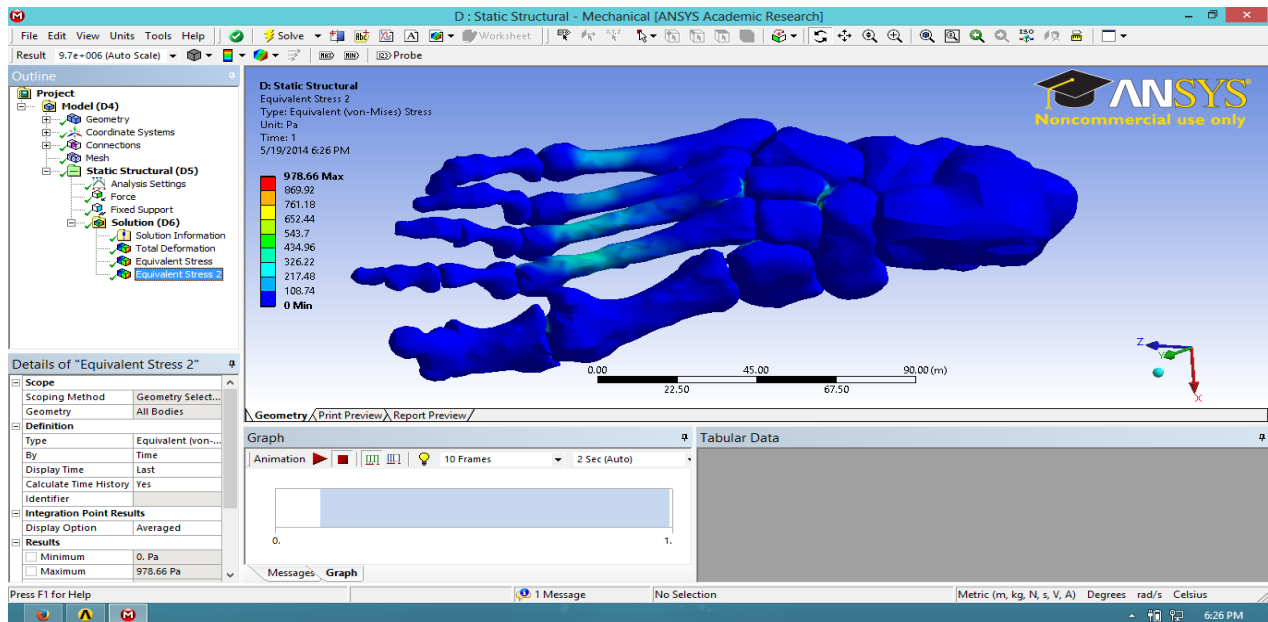


Fig. 4.19 Screenshot of Von-Mises stress of foot model by applying 600N at an angle 90°

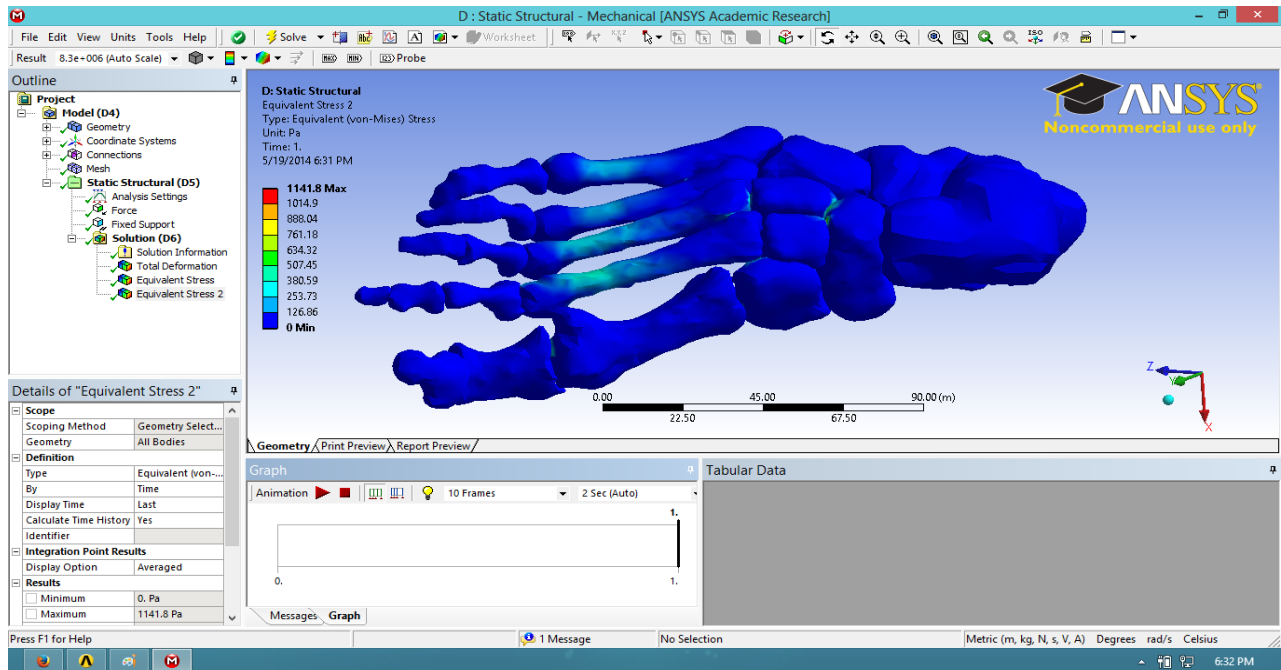


Fig. 4.20 Screenshot of Von-Mises stress of foot model by applying 700N at an angle 90°

Finally Von-Mises stress was calculated by applying 800N. The numerical values of maximum Von-Mises stress were found to be at a maximum of 1304.9 Pa and minimum of 0 as shown in Fig. 4.21.

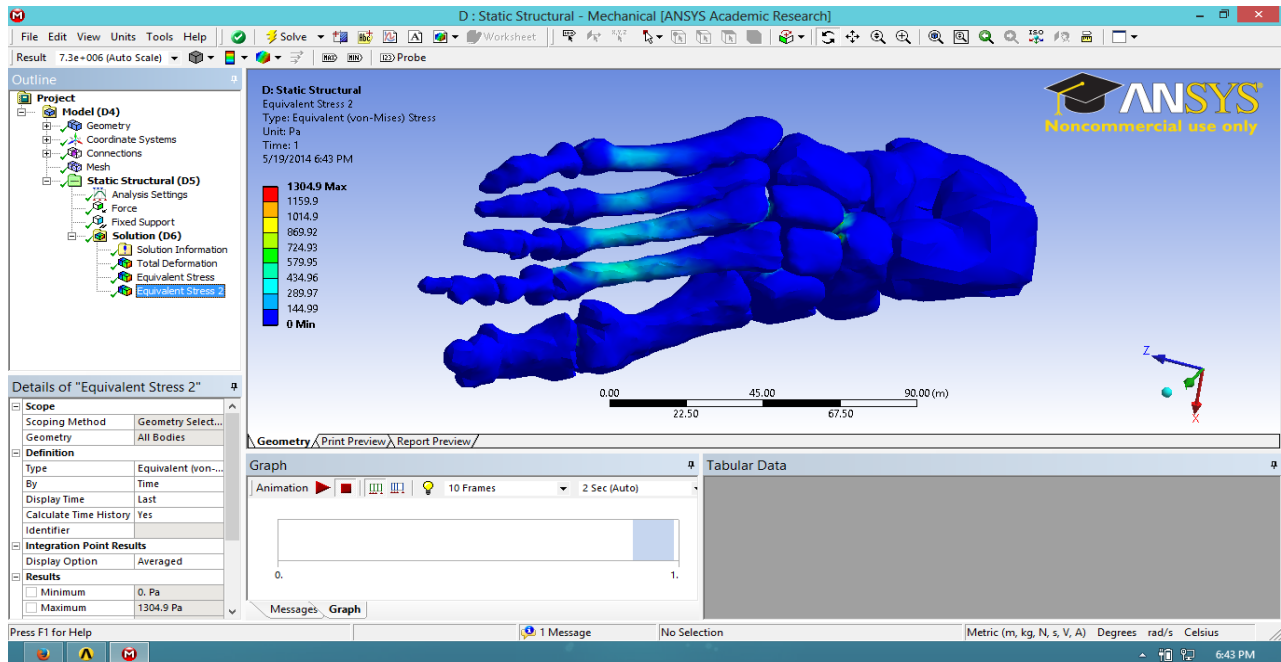


Fig. 4.21 Screenshot of Von-Mises stress of foot model by applying 800N at an angle 90°

By applying 600N at angle of 120^0 the Von-Mises stress was found to be 459.99 Pa as shown in Fig.4.22. From the colour distortion in the figure it is observed that the stress value is very less.

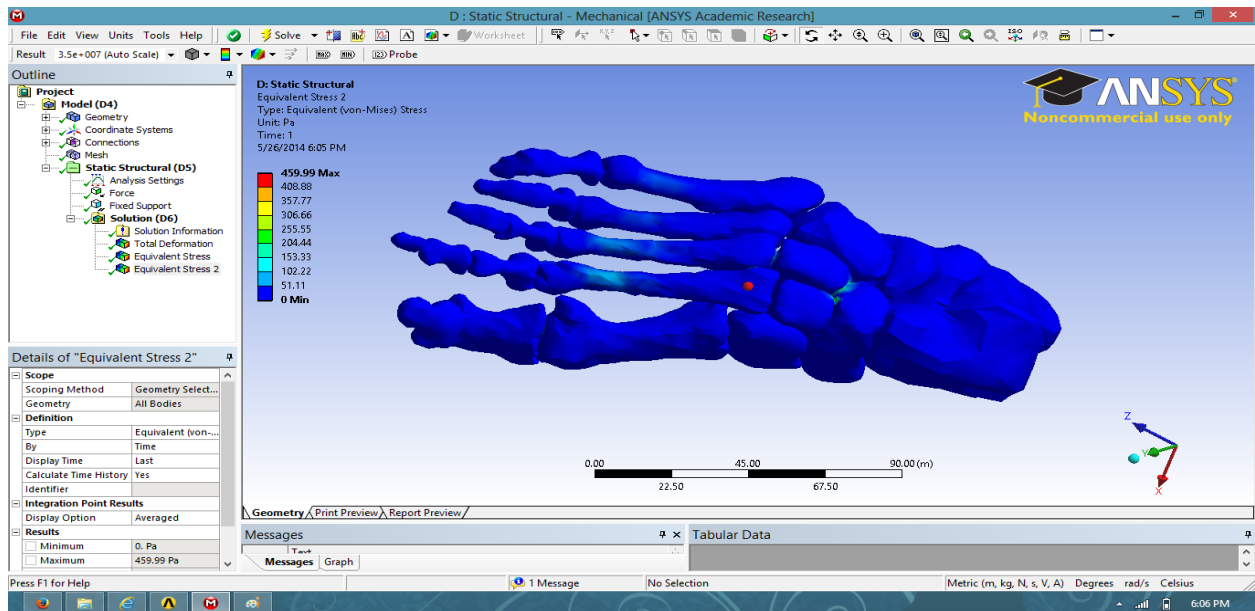


Fig. 4.22 Screenshot of Von-Mises stress of foot model by applying 600N at an angle 120^0

Similarly by applying 700N at angle of 120^0 the maximum Von-Mises stress was found to be 536.66 Pa and the minimum Von-Mises stress was 0 as shown in Fig.4.23. In this case also the observed regions of colour distortion is limited.

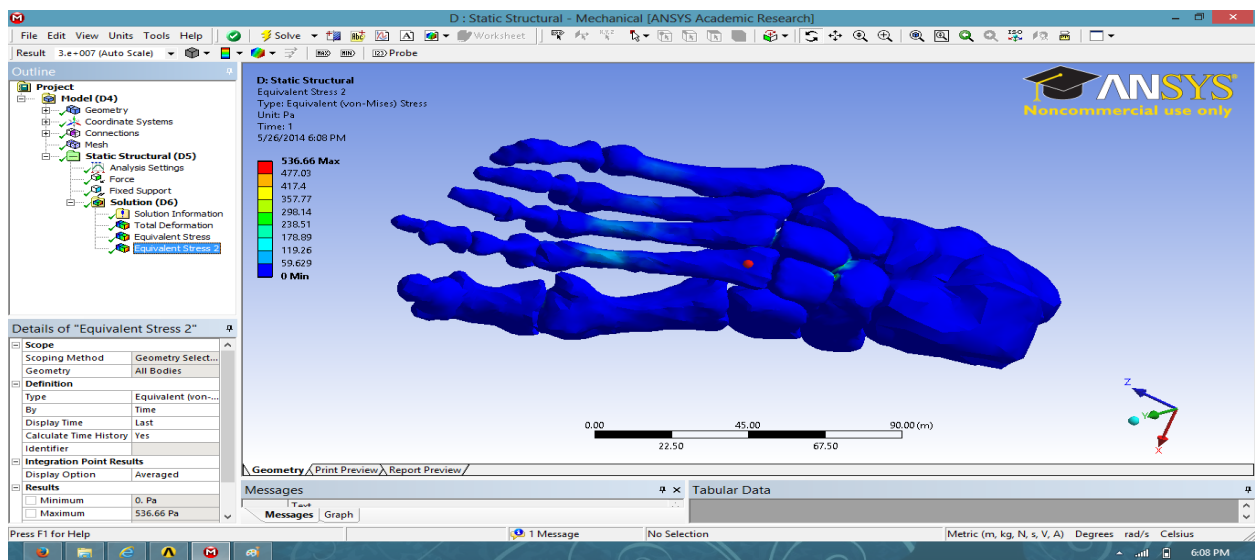


Fig. 4.23 Screenshot of Von-Mises stress of foot model by applying 700N at an angle 120^0

By applying 800N at angle of 120° the maximum Von-Mises stress was found to be 613.3 Pa and the minimum Von-Mises stress was 0 as shown in Fig.4.24. In comparison to the above two figures the maximum magnitude of stress in this case is largest.

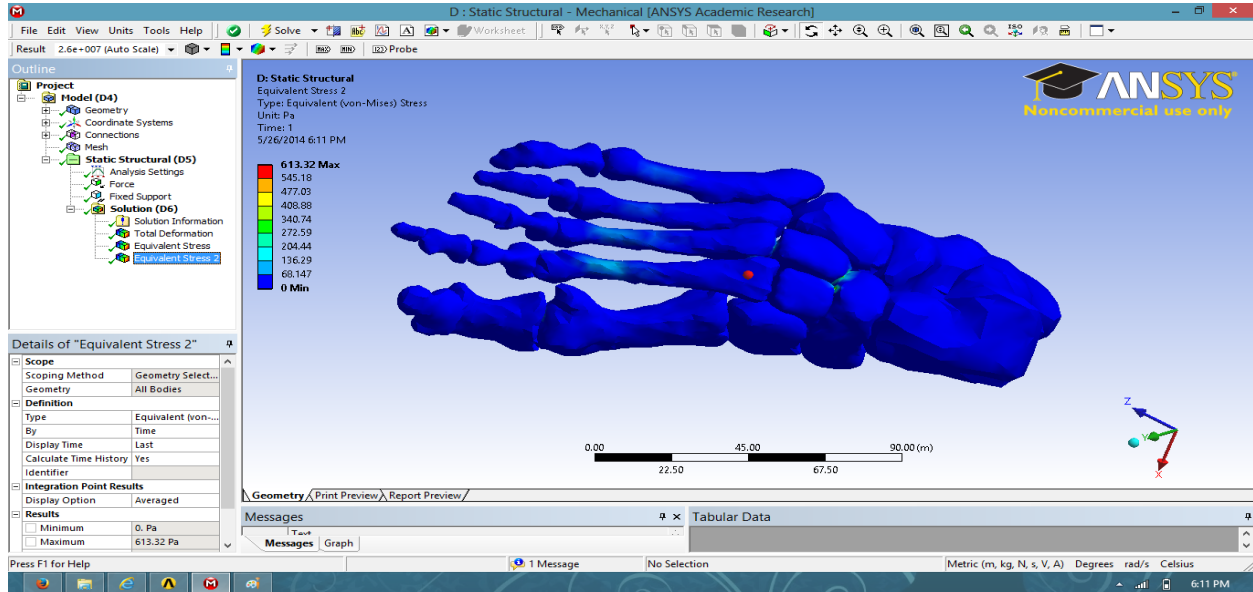


Fig. 4.24 Screenshot of Von-Mises stress of foot model by applying 800N at an angle 120°

By applying 600N at angle of 45° the maximum Von-Mises stress was found to be 412.98 Pa as shown and the minimum Von-Mises stress was 0 in Fig.4.25.

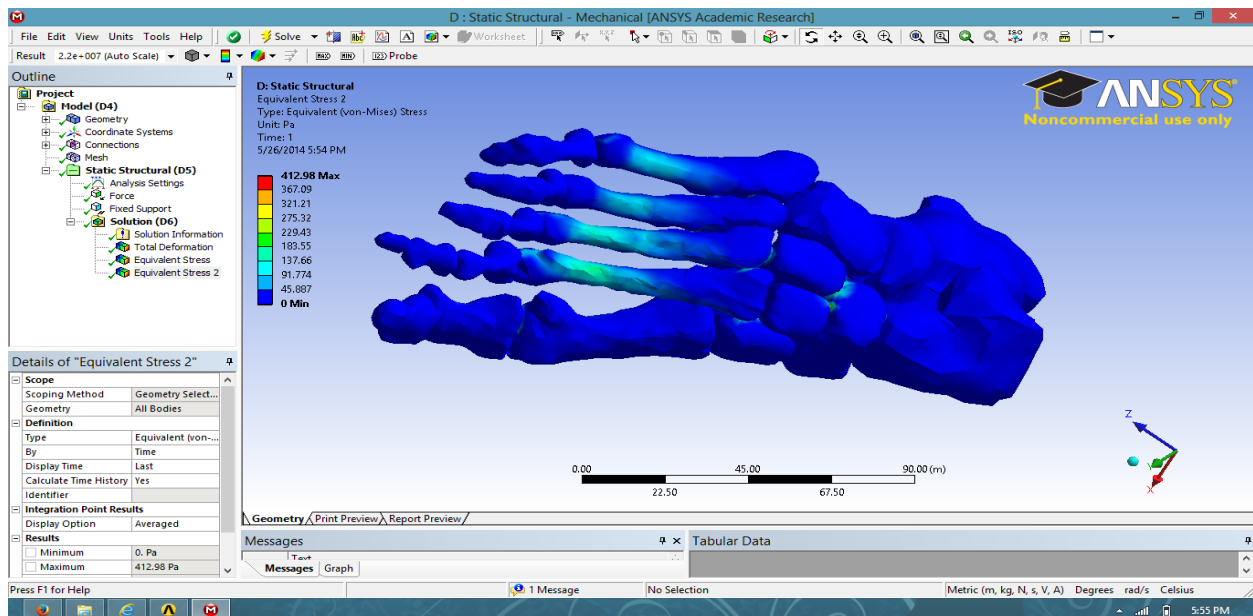


Fig. 4.25 Screenshot of Von-Mises stress of foot model by applying 600N at an angle 45°

By applying 700N at angle of 45° the maximum Von-Mises stress was found to be 481.81 Pa and the minimum Von-Mises stress was 0 as shown in Fig.4.26.

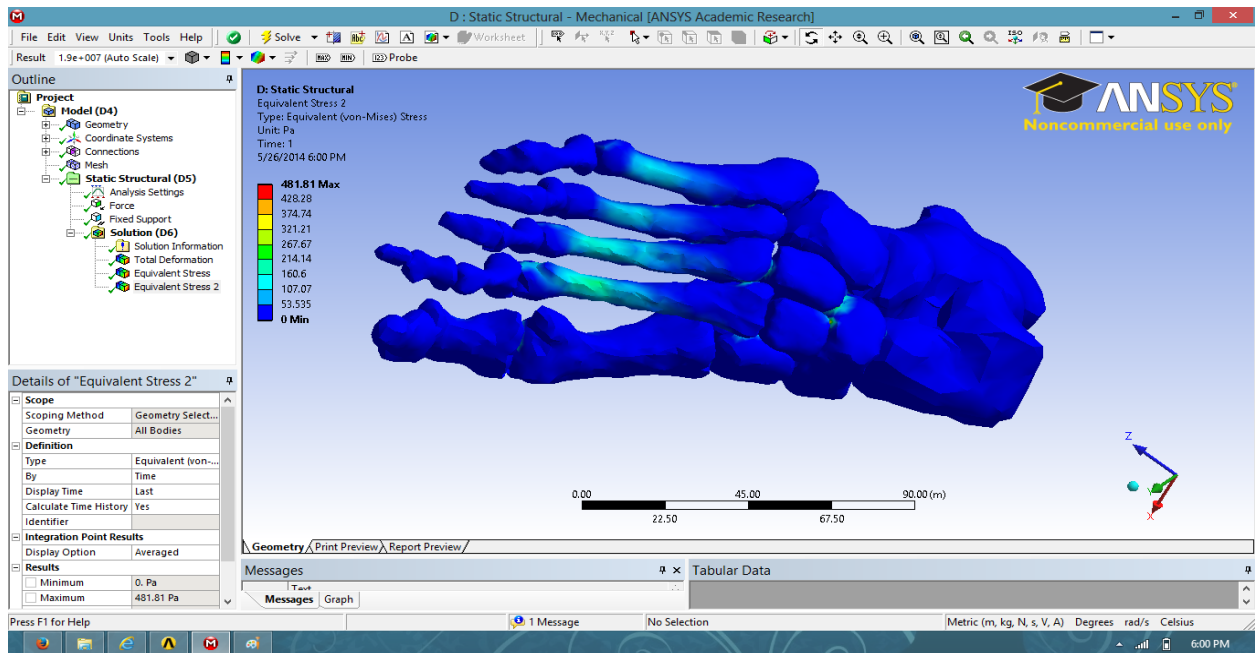


Fig. 4.26 Screenshot of Von-Mises stress of foot model by applying 700N at an angle 45°

By applying 800N at angle of 45° the maximum Von-Mises stress was found to be 550.64 Pa and the minimum Von-Mises stress was 0 as shown in Fig.4.27.

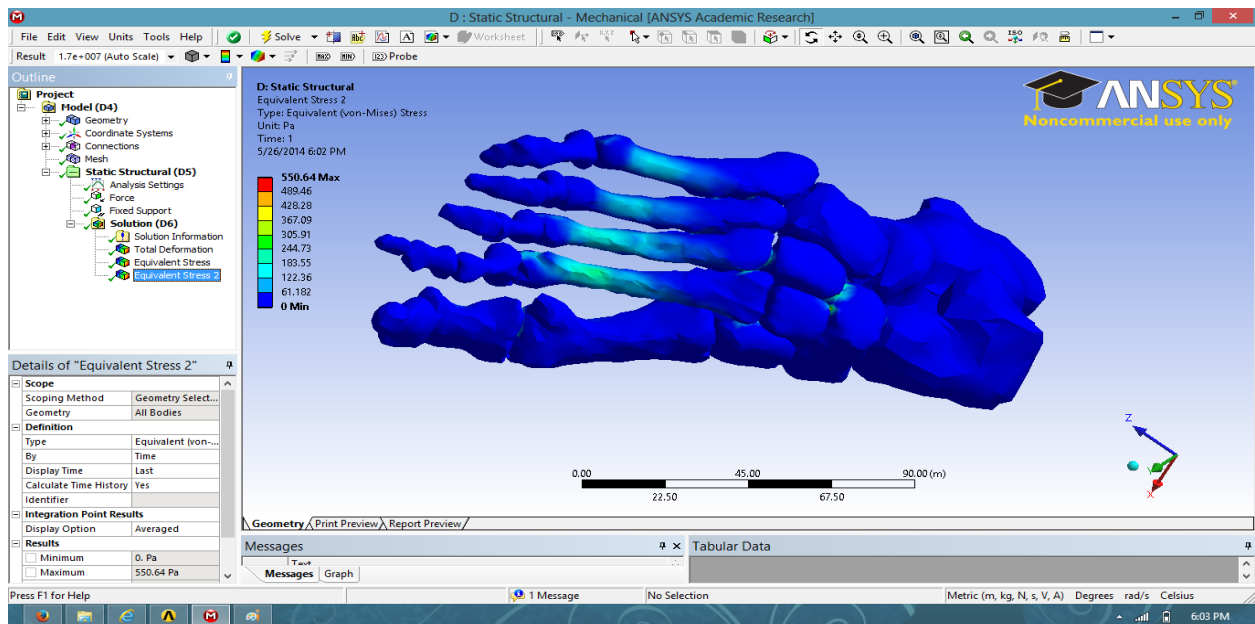


Fig. 4.27 Screenshot of Von-Mises stress of foot model by applying 800N at an angle 45°

Table 4.1 Results of the maximum deformation and stress obtained for different values of forces acting on the same joint at three different angles.

Force Acting (in N)	Maximum deformation (in m)			Maximum Stress (in Pa)		
	45 ⁰	120 ⁰	90 ⁰	45 ⁰	120 ⁰	90 ⁰
600	0.03965	0.025806	0.053553	412.98	459.99	978.66
700	0.04626	0.030107	0.062478	481.81	536.66	1141.8
800	0.05287	0.034408	0.066941	550.64	613.3	1304.9

The data in the [Table 4.1](#) shows that the variation of magnitude of deformation and stress of the bone follows the following trend:

- For a constant angle of application of force, the maximum value of stress and deformation varies almost linearly, since $\sigma \propto F$ and $\Delta L \propto F$, where σ is the stress, F is the force acting and ΔL is the change in length. And $F \propto MA$, M is the mass and A is the acceleration. So the stress distribution in the foot depends on the mass, geometry and structure of the footmodel.
- For a constant force, acting at different angles it is observed that magnitude of stress increases non-linearly with change in angle of application of force, whereas the trend of variation of maximum deformation value shows a drop in value at an angle of 120⁰ as compared to the values at 45⁰ and 90⁰.
- Both the total deformation and stress is maximum when load on the foot has an angle of 90⁰ with the horizontal.
- Total deformation was minimum while descending a slope at an angle of 120⁰, but stress was minimum during ascending or climbing a slope at an angle of 45⁰. The variations of total deformation and stress were indicated by different colours.

5.0 SUMMARY AND CONCLUSION

The finite element methodology is a powerful method to grasp the foot mechanical behavior and its implication in studying the foot comfort. An anatomically elaborated foot model of human was generated from CT images information using segmentation reconstruction techniques and 3D CAD modeling software.

The 3D model of human foot bone was constructed by using various softwares. Then deformation and stress analysis was performed using ANSYS. The total deformation and stress was calculated by applying various types of loads in different angles.

The maximum deformation value is obtained at the calcaneus portion of foot and it gradually decreases towards the fore foot. Rear foot has more deformation than fore foot. During descending a slope the foot has more deformation than ascending an angle of 120° . In all the cases, the minimum deformation was found to be 0. From the above experiment, it is observed that the deformation increases gradually with increase in loads. Similarly, stress was calculated by applying various forces. The corresponding stress values also increased with application of larger values of forces. The stress in metatarsal bones is found to be more, while minimum in phalanges.

From trend of values it can be deduced that the total deformation is minimum when force acts at an angle of 120° on the ankle joint, and the deformation has maximum magnitude at an angle of 90° . Hence, it can safely deduce that the heel strike at an angle of 90° should be avoided, as it might give rise to chronic problems such as planter fasciitis, arthritis, heel spurs, stress fracture and bursitis. This has a great significance for sports persons (sports biomechanics). The heel strike angle should be kept less than 90° and above or equal to 120° for painfree performance.

REFERENCES

REFERENCES

- [1] T. Asai and H. Murakami, "Development and Evaluation of a Finite Element Foot Model", Proc. of the 5th Symp. on Footwear Biomechanics, 2001, Zuerich / Switzerland, pp. 10-11.
- [2] J. K. Aggarwal and Q. Cai, "Human Motion Analysis A Review", Computer Vision and Image Understanding, 73(3), March 1999, pp. 428-440.
- [3] L. Bustillos, L. Derikx, N. Verdonschot, N. Calderon and D. Zurakowski, "Finite Element Analysis And CT-Based Structural Rigidity Analysis To Assess Failure Load In Bones With Simulated Lytic Defects", Bone, 58, January 2014 , pp.160-167.
- [4] J. Cheung, M. Zhang, A. Leung and Y. Fan, "Three-Dimensional Finite Element Analysis of the Foot During Standing-A Material Sensitivity Study", Journal of Biomechanics, 38(5), May 2005, pp. 1045-1054.
- [5] P.J. Antunes and G. R. Dias, "Nonlinear 3D Foot FEA Modelling from CT Scan Medical Images", Materials Science Forum, 700, 2011, pp. 135-141.
- [6] A. Chawla, S. Mukherjee and G. Sharma, "Finite Element Meshing of Human Bones from MRI/CT Raw Data", Journal of Mechanics in Medicine and Biology, 2006, New Delhi, pp. 1-9.
- [7] M.A. Kumbhalkar, U. Nawghare, R. Ghode, Y. Deshmukhand B. Armarkar, "Modeling and Finite Element Analysis of Knee Prosthesis With and Without Implant", Universal Journal of Computational Mathematics, 1(2), 2013, pp. 56-66.
- [8] Ir. P. Boeraeve, "Introduction to the Finite Element Method (FEM)", Institutgramme Liege, January 2010, pp. 2-68.
- [9] D. Roylance, "Finite Element Analysis", Department of Materials Science and Engineering Massachusetts Institute of Technology, Cambridge, MA 2139, February 2001, pp. 1-16.
- [10] Z. Qian, L. Ren and Y. Ding, "A Dynamic Finite Element Analysis of Human Foot Complex in the Sagittal Plane during Level Walking", Plos one, 8(11), November 2014, pp. 1-10.
- [11] T. Qiu, E. Teo, Y. Yan and W. Lei, "Finite Element Modeling of a 3D Coupled Foot Boot Model", Medical Engineering and Physics, 33(10), December 2011, pp. 1228-1233.

- [12] S.H. Kim, J.R. Cho, J.H. Choi, S.H. Ryu and W.B. Jeong, “Coupled Foot-Shoe-Ground Interaction Model To Assess Landing Impact Transfer Characteristics to Ground Condition”, *Interaction and Multiscale Mechanics*, 5(1), 2012, pp. 75-90.
- [13] Biomechanics of running, www.pt.ntu.edu.tw/hmchai/BM03/BMsports/Run, 2014.
- [14] Basic Anatomical Terms and Definitions, www.footdoc.ca/ www.FootDoc.ca/Website%20Definitions%20%28Basic%20Terms%29, 2014.
- [15] J. Cheung, and M. Zhang, “A 3-Dimensional Finite Element Model of the Human Foot and Ankle for Insole Design”, *Academy of Physical Medicine and Rehabilitation*, 86, February 2005, pp. 353-358.
- [16] A. Gefen, “Stress Analysis of The Standing Foot Following Surgical Plantar Fascia Release”, *Journal of Biomechanics*, 35,2002, pp. 629–637.
- [17] M. Ozen, O. Sayman and H.Havitcioglu,” Modeling And Stress Analyses of A Normal Foot-Ankle And A Prosthetic Foot-Ankle Complex”, *Acta of Bioengineering and Biomechanics*,15(3), 2013, pp. 19-27.
- [18] S.H. Kim, J.R. Cho, J.H. Choi, S.H. Ryu and W.B. Jeong, “Coupled Foot Shoe Ground Interaction Model to Assess Landing Impact Transfer Characteristics to Ground Condition”, *Interaction and Multiscale Mechanics*, 5(1), 2012, pp. 75-90.
- [19] R. Stallman, “Numerical Modeling of Human Foot”, *Journal of Biomechanical Engineering*, 2, 2013, pp. 29-55.